Characterization of Protein Release from Poly(ethylene glycol) Hydrogels with Permeability Gradients

by

Tuğba Bal

A Thesis Submitted to the
Graduate School of Engineering
in Partial Fulfillment of the Requirements for
the Degree of

Master of Science
in
Chemical and Biological Engineering

Koc University

August 2012

Koc University

Graduate School of Sciences and Engineering

This is to certify that I have examined this copy of a master's thesis by

Tuğba Bal

and have found that it is complete and satisfactory in all respects,
and that any and all revisions required by the final
examining committee have been made.

Committee Members:

_____

Seda Kızılel, Ph. D. (Advisor)

_____

Can Erkey, Ph. D.

_____

Murat Sözer, Ph. D.

Date: 08/29/2012

ABSTRACT

PEG [poly(ethylene glycol)] hydrogels have been applied as carriers and/or supporting scaffolds in many areas including biomedicine, biotechnology and membrane science due to their biocompatibility, nontoxicity, permselectivity and tunable properties. In this study, physical properties of PEG hydrogels were tuned by molecular weight and concentration of PEGDA monomer in the resulting hydrogel network and effect of such changes on protein release and cytocompatibility were investigated. For this purpose, in the first step, PEG hydrogels were formed by surface initiated photopolymerization and swelling experiments were performed. Obtained data were used to estimate physical properties including mass and volumetric swelling ratio, molecular weight between crosslinks and mesh size. The inverse relations between physical properties and concentration of PEGDA were obtained. Further, it was concluded that PEGDA molecular weight positively regulates physical properties. In the following step, BSA and GLP-1 (9-37) were used as model biomolecules to get insight into the release behavior of physically entrapped molecules from PEG hydrogel formed by surface initiated photopolymerization. The diffusion experiments showed that BSA and GLP 1(9-37) can be released from PEG hydrogels depending on both solute and network properties such as solute size and molecular weight, swelling ratio and mesh size. In the last part, hydrogels with or without RGDS functionality were synthesized to determine cytocompatibility of the applied system. It was showed that this system can support fibroblast viability regardless of molecular weight and concentration of PEGDA. In conclusion, PEG hydrogels synthesized here are applicable for controlled release of bioactive molecules and cell based studies.

ÖZET

PEGDA [poli(etilen glikol)] sujelleri biyotıp, biyoteknoloji ve membran bilimleri gibi bir çok alanda biyouyumlu, serçici geçirgen olmaları, toksik olmamaları ve değiştirilebilir özelliklere sahip olmalarından dolayı taşıyıcı ve/veya destekleyici yapı iskeleleri olarak kullanılmaktadır. Bu çalışmada, PEG sujellerinin fiziksel özellikleri PEGDA monomerinin moleküler ağırlığına ve konsantrasyonuna bağlı olarak control edildi ve bu tür değişikliklerin protein salımına ve hücre uyumluluğuna etkisi incelendi. Bu amaçla, ilk aşamada, PEG sujelleri yüzeyden başalayan fotopolimerizasyon ile oluşturuldu ve su alımı deneyleri yapıldı. Elde edilen veriler kütlesel ve hacimsel su alımı, çapraz bağlar arasındaki moleküler ağırlık ve por boyutunu hesaplamak icin kullanıldı. Fiziksek özellikler ile PEGDA konsantrasyonu arasında ters ilişki elede edildi. Ayrıca, PEGDA'nın moleküler ağırlığının fiziksel özellikleri olumlu yönde etkiledigi gözlendi. Bir sonraki aşamada, BSA ve GLP1 (9-37) yüzeyden başlayan fotopolimerizasyon ile oluşturulan PEG sujelinden fiziksel olarak hapsedilmiş moleküllerin salım davaranışını inclemek icin model biyomoleküller olarak kullanıldı. Difüzyon deneyleri BSA ve GLP1 (9-37)'nin PEG sujellerden çözünen madde büyüklüğü ve moleküler ağırlığı, su alım miktarı ve por boyutu gibi hem çözünen madde hem de ağ özelliklerine bağlı olarak salınabileceğini gösterdi. Son bölümde, RGDS içeren ve içermeyen PEG sujelleri, uygulanan sistemin hücre uyumluluğunu test etmek için kullanıldı. Bu sistemin fibrablast yaşayabilirliğini PEGDA moleküler ağırlığı ve konsantrasyonuna bağlı olmadan destekleyebileceği gösterildi. Sonuç olarak, bu çalışmada elde edilen PEG sujelleri biyoaktif moleküllerin kontrollü salımı ve hücresel çalışmalarda kullanılabilir.

ACKNOWLEDGEMENTS

I would like to thank to Assist. Prof. Dr. Seda Kızılel for her support, thought-provoking suggestions and her assistance to frame the ideal environment to get new insights about my career. She shared a large part of her time for directing me about my experimental plan and discussions on the results. I sincerely appreciate for letting me study under her support and encouragement during my master. I am also grateful to her for supporting me to perform research at University of Chicago about insulin secreting islet cells.

I also would like to thank my committee members, Prof. Dr. Can Erkey and Assoc. Prof. Dr. Murat Sözer for being a part of my thesis committee.

I would like to thank the Scientific and Technological Research Council of Turkey (TUBITAK) for MS scholarship.

I am glad to be a part of our laboratory group. Tthanks to my laboratory colleagues, Selin Kanyas, Selimcan Azizoğlu and Burcu Kepsutlu for enjoyable lab hours, advices and motivation. I am grateful to Selma Bulut and Hande Asımgil for support and advices on keeping cells. I wish all the best positions in their lives.

Finally, I would like to thank to my family for the opportunity of motivation and support that directed and stimulated my interests during my master study. I could not manage whole my study without them. I am grateful to my sister, Bilge for her help in drawings.

TABLE OF CONTENTS

LIST OF TABLES

LIST OF FIGURES

ABBREVIATIONS

FDA	Food and Drug Administration
DNA	Deoxyribonucleic acid
PEG	Poly(ethylene glycol)
PEGDA	Poly(ethylene glycol) diacrylate
BSA	Bovine serum albumin
GLP1 (7-37)	Glucagon like peptide 1 (7-37)
VEGF	Vascular endothelial growth factor
pNIPAAM	Poly(N-isopropylacrylamide)
RGDS	Arg-Gly-Asp-Ser
ECM	Extracellular matrix
PEO	Poly(ethylene) oxide
HUVEC	Human umbilical vein endothelial cells
MMP	Matrix metalloproteinase
bFGF	Basic fibroblast growth factor
PLGA	Poly(lactic-co-glycolic acid)
GLP1 (9-37)	Glucagon like peptide 1 (7-37)
HSA	Human serum albumin
PVA	Poly(vinyl) alcohol
DDP-4	Dipeptidyl peptidase-4
UV	Ultraviolet
TEA	Triethanolamine
NVP	1-vinyl-2-pyrrolidinone
PDB	Pendant double bond
acr-PEG-NHS	Acrylate-PEG-N-hydroxysuccinimide

DMEM	Dulbecco's Modified Eagle Medium
FBS	Fetal bovine serum
EDTA	Ethylenediaminetetraacetic acid
PBS	Phosphate buffered saline

NOMENCLATURE

M_c	Molecular weight between crosslinks
q	Mass swelling ratio
W_s	Weight at swollen (wet) state
W_d	Weight at dry state
Q	Volumetric swelling ratio
ρ_s	Density of the solvent (water)
ρ_p	Density of the polymer (PEG)
M_n	Chain length of the starting polymer
χ	Flory interaction parameter
$\bar{\upsilon}$	Specific volume of the polymer
V_1	Specific volume of solvent
$v_{2,r}$	Polymer volume fraction of the hydrogel in the relaxed state
$v_{2,s}$	Polymer volume fraction of the hydrogel in the swollen state
V_d	Volume of the dry polymer sample
V_o	Gel sample volume before equilibrium swelling
V_s	Gel sample volume after equilibrium swelling
$(r_o^{-2})^{1/2}$	Root mean squared end-to-end distance of the unperturbed (solvent-free) state
l	Bond length
M_r	Molecular weight of PEG repeat unit
C_n	Characteristic ratio for PEG
ξ	Mesh size
D_0	Diffusivity in water
η	Viscosity of water

R_s	Solute radius
k	Boltzman's constant
T	Temperature
M_i	Mass released at time i
C_i	Concentration of solute at time i
V	Volume of the solution
V_s	Sample volume
M_{inf}	Initial protein mass
D_e	Effective diffusion coefficient
t	Time
δ	Hydrogel thickness

Chapter 1

INTRODUCTION

Hydrogels are water swollen networks that have created great interest due to their high water content, biocompatibility and especially their mechanical and chemical similarity to the natural environment of the cells. So far, they have been used for cell, bioactive molecule and DNA delivery, in dental materials and as biosensors.[1-4] In cell and drug delivery areas, promising studies led to the growth of "gradient hydrogels" to mimic cell behavior and fate of the natural extracellular matrix. Controlled delivery studies have also been conducted with gradient hydrogels. [5]

Recently, synthetic hydrogels composed of poly(ethylene glycol) diacrylate were used in tissue engineering and drug delivery applications extensively because of their non-immunogenicity, biocompatibility, nontoxicity and tunable properties. Additionally, they have been approved by the FDA.[6, 7] PEG incorporated hydrogels are applied as carriers to release molecules including bovine serum albumin, vitamin B12, ovalbumin, lysozyme, immunoglobulin G, insulin, myoglobin and the vascular endothelial growth factor.[8-11] In addition to therapeutic studies, PEG hydrogels have been considered as platforms to promote vascularization, to provide immunoprotection of pancreatic islets from immune system, and for fibroblast migration and proliferation.[12-15]

In recent studies, gradient hydrogels have been generated with microfluidic devices via a two-step approach, either with chemical or physical gradients. In these systems, gradients were formed and stabilized by crosslinking.[5] For example, Delong et al. used a gradient maker to form concentration gradients of RGDS on the PEG hydrogel surface

to direct fibroblast migration and alignment.[16] In 2009, Nemir et al. produced an elasticity gradient in PEG hydrogels by mixing two different molecular weights of PEGDA with a gradient maker to asses mechanical and swelling properties and they also applied patterned elasticity to determine macrophage adhesion.[17] Instead of using a two step approach, in 2004, Kızılel and her colleagues developed a novel technique with PEGDA to form PEG hydrogels with a permeability gradient.[6] This procedure allows for the synthesis of hydrogels with permeability gradients using a single photopolymerization step. With this technique, it is also possible to study controlled drug and protein delivery as well as cell-matrix interactions such as matrix remodeling, migration and differentiation in 2D and 3D environments. Semi-permeable barriers can be formed with these networks to control diffusion of molecules while preventing immune rejection and cell leakage. Also, these networks can be used to generate covalent gradients of bioactive molecules such as GLP-1 (7-37). [18, 19]

In this thesis, chapter 2 provides an overview on recent advances in cell and drug delivery from PEG hydrogel networks to give general information. The chapter includes PEG hydrogel properties, synthesis and applications in drug delivery and tissue engineering applications. Also, it addresses significance of permeability and cytocompatibility of PEG and other hydrogel networks.

Chapter 3 presents materials and methods used in experimental part of this thesis. In the beginning of chapter 3, PEG hydrogels having permeability gradients were synthesized by surface initiated photopolymerization in a single step to characterize their properties. For this purpose, swelling experiments were performed to calculate swelling ratio, molecular weight between crosslinks (M_c) and mesh (pore) size, since these properties determine transport properties of the membrane. Swelling experiments were performed to estimate permeability properties of hydrogels formed with various PEGDA molecular weights and concentrations.

Chapter 3 also explains how PEG hydrogels were synthesized for controlled release of bovine serum albumin (BSA) and GLP-1 (9-37). This type of release can be used for site-specific drug or bioactive molecule delivery without adverse effects on bolus injection and can be used to form therapeutic agent gradients in hydrogel. Further, it provides information about molecule size that can pass through PEG membrane. These results can be considered for immunoprotection and permeability capacity of PEG hydrogel.

In the last part of the chapter, PEG hydrogels were functionalized with RGDS peptide to enhance cell adhesion. Viability assays with fibroblasts were performed to determine the cytocompatibility of the system, since proof of the nontoxicity of the system is required for applicability in biological systems.

Following chapter 4 with the results and discussion, this thesis ends with Chapter 5 by summarizing conclusion and future work that can be carried out using the proposed system.

Chapter 2

LITERATURE REVIEW

2.1. Hydrogels

2.1.1. Hydrogels: Properties and Applications

Hydrogels are water swollen networks that absorb large quantities of water without showing dissolution profile in water (i.e. insoluble in water) due to physical or chemical crosslinks provided for integrity. These three dimensional networks can absorb water by hydrophilic side groups such as –OH, -CONH-, -$CONH_2$-, -COOH and -SO_3H.[1, 20] After Wichterle and Lim developed poly (2-hydroxyethyl methacrylate) gels for contact lenses in the 1960s,[4] hydrogels created great interest in both tissue engineering and drug delivery applications due to their biocompatibility and water content as well as mechanical, compositional and physicochemical similarity to the extracellular matrix.[1-4]

When treatment of a disease with cell transplantation is used as strategy, direct injection causes rapid immune response, thus cell viability and graft success decrease. Immunosuppressive drugs can also be used with transplanted cells, but this increases tendency to get other infections. Instead, encapsulating cells in hydrogels is a promising strategy to limit access of immune cells and to mechanically support cells. These all increase efficacy and viability of transplanted cells and control is possible by material immunogenicity and porosity. So far, hydrogels are applied for cell studies such as islets,

nerve, cartilage, liver and cornea as well as DNA, growth factor, protein and drug delivery.[2, 18, 21] In such studies, it is also proven that hydrogels are good candidates as drug and protein carriers, since they do not destroy structure and therapeutic functionality of the drug/protein.[9] For example, Zisch and his colleagues covalently immobilized vascular endothelial growth factor to proteolytically degradable PEG hydrogel and showed that as the matrix was cleaved by cells, released protein induced vascularization in implanted site in adult rat models.[22] In another study, Kızılel and her colleagues used PEG multilayers formed by surface initiated photopolymerization with a photomask. This application is a useful tool to study cell behavior in 2D. [23]

For these applications, polymers used in hydrogel chemistry are either natural or synthetic. Naturally derived hydrogels are mostly composed of hyaluronic acid, fibrin, alginate, collagen, dextran, chitosan, gelatin and agarose. They are good carriers because of inherent properties such as proteolytic degradation, biological recognition and remodeling. Purification, insufficient mechanical properties, batch-to-batch differences, uncontrollable mechanical and biochemical properties, immunogenicity and disease transmission capacity of natural materials cause severe problems in biomedical applications.[21, 24-27]

In contrast, polymers applied in synthetic networks are mostly formulated with monomers such as poly(ethylene glycol), poly(vinyl) alcohol, hydroxymethyl methacrylate, N-isopropyl acrylamide and poly(acrylic) acid. Synthetic hydrogels are produced under mild conditions, they are biocompatible and posses tailorable properties. For example, a porous structure can be tuned by changes in the number of crosslinks. Furthermore, the manufacturing process for synthetic hydrogels is highly reproducible and synthetic hydrogels can be modified to gain some properties that provide some benefits.[21, 26, 28] For instance, depending on the application, hydrogels are designed as enzymatically, hydrolytically or environmentally (e.g. pH, temperature, electric field)

degradable.[28] In such studies, Seliktar and his colleagues developed enzyme sensitive biocompatible PEG hydrogel to deliver the vascular endothelial growth factor (VEGF) for vascular healing and visualized cell attachment.[29] Drapala et al. established thermo-responsive poly(N-isopropylacrylamide) (pNIPAAm) hydrogels and applied them for controlled release of bovine serum albumin.[30] Alternatively, magnetic or electric field, glucose, urea, pH, temperature, morphine and antibody sensitive hydrogels are currently being studied for various applications.[4] Also, synthetic hydrogels can be modified to have adhesion sites for a wide variety types of cells such as osteoblasts, fibroblasts, smooth muscle, epithelial and endothelial cells to study cell behavior.[31, 32] As an example, Burdick et al. proposed mineralization and differentiation of osteoblast due to the osteoblast like growth factor released from degradable RGDS functionalized PEG hydrogels.[33]

Hydrogels are designed with chemical or physical crosslinks. Chemical crosslinks are compromised of covalent bonds. They are generated by radical polymerization, chemical reaction of complementary groups, high energy irradiation and by using enzymes. Physical crosslinks are entanglements, crystallites and weak bonds such as Van der Waals interactions and hydrogen bonds. Physical links can be introduced to the network structure by ionic interactions and hydrogen bonds.[1, 34, 35]

Hydrogels are usually formed with homopolymers or copolymers and are classified according to a wide variety of criteria including charge, morphology and network structure. Side groups render them as neutral or ionic networks. Also, based on morphology, they are classified as supermolecular structures, hydrocolloidal aggregates, amorphous, semicrystalline and hydrogen bonded structures. Additionally, alterations in network structure divide hydrogels into three groups: Nonporous, microporopous and macroporous.[1]

Porosity property has a profound effect on nanoscopic properties of hydrogels, since by adjusting permeability by porosity, semi-permeable barriers can be formed to control diffusion of molecules/metabolites and nutrients/wastes while preventing immune rejection and cell leakage (Figure 2.1). [18, 36] Moreover, drug loading and cell behavior such as migration, differentiation, proliferation, tissue regeneration and apoptosis can be dictated by permeability, mechanical and biochemical properties.[5] In drug eluting systems, controlled sustained site specific release is governed by pore sizes and crosslink density.[28] This parameter can be adjusted with changes in backbone chemistry of polymeric materials or physical properties of hydrogels. For instance, hydrophilicity of the groups can be increased to enhance mass transport. It is also possible to remodel compositions of initial monomers and their ratios, crosslink density, molecular weight and concentration of polymeric material, functional group density and polymerization conditions to control permeability by pore (mesh) size, network structure and swelling. [36]

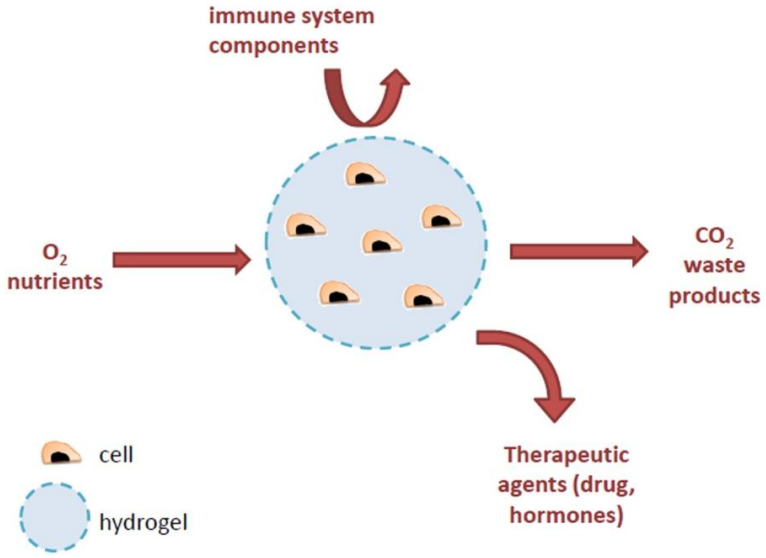

Figure 2.1. Semi-permeable membrane for tissue engineering and therapeutic agent delivery

Beyond these studies, for the last few years, there have been noticeable attempts to produce hydrogels with chemical or physical "gradients". These attempts were inspired from the nature of extracellular matrix (ECM). ECM presents physical, chemical and mechanicals guides to determine cell fate and to regulate migration, proliferation and interaction. The gradient cues drive processes such as morphogenesis, chemotaxis, embryogenesis and wound healing. These gradients are used to get detailed insights about cell-biomaterial interaction and other cellular processes. Moreover, both in tissue engineering and drug delivery approaches, gradients are applied to mimic ECM and control the release of molecules.[5] Gradients are formed by gradient photo-crosslinking methods and microfluidic devices. The chemical gradients in hydrogels are composed of immobilized peptide/proteins and soluble growth factor gradients. Physical gradients cover stiffness, pore size and porosity gradients and are favorable for studying the processes of mechanotransduction and cell behavior.[5]

2.1.2. PEG Hydrogels

2.1.2.1. PEG Hydrogel Properties

Poly(ethylene glycol) (PEG) (Figure 2.2) is a non-immunogenic, biocompatible, hydrophilic, nontoxic, branched or linear, FDA approved polyether with tunable properties.[6, 37, 38] "PEG" is used for molecular weights less than 20 kDa whereas higher molecular weights are known as "PEO [poly(ethylene) oxide]".[7] When PEG is converted into hydrogels, it presents ester bonds for hydrolysis.[39] The characteristics of PEG are influenced by molecular weight and chain shape. Molecular weights less than 400 Da PEGs are oil. Those between 1.5-2 kDa PEGs have a waxy appearance, and higher molecular weights are in powder form. PEGs are sensitive to oxidation resulting chain cleavage, so they should be stored under inert atmosphere.[40]

PEG is synthesized by acyclization of ethylene oxide and used for the production of PEG derivatives such as PEG diacrylate (Figure 2.3) and PEG dimethacrylate.[41, 42] These PEG derivatives, modified with adhesive ligands, growth factors and degradable sequences,[43-45] are synthesized to obtain desired properties in various applications including medical devices, implants, drug and gene delivery.[7] Furthermore, it is applied in some FDA approved or advanced clinical trials of proteins and oligonycleotides in hepatitis C, rheumatoid arthritis, anemia and several other diseases. [40]

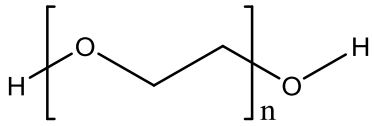

Figure 2.2. Structure of PEG [poly(ethylene) glycol]

PEG acts as a blank state and thus resists absorption of proteins and prevents immune response. This bioinertness is the result of osmotic and entropic properties based on steric repulsion of hydrated PEG chains. The ethylene oxide units in PEG provide hydrophobicity whereas as oxygen units interact with water molecules. With this unique behavior, PEG can be dissolved both in water and organic solvents.[7, 40] Also, it has high water content similar to extracellular matrix properties, which makes PEG desirable to use in cell-based therapies.[6]

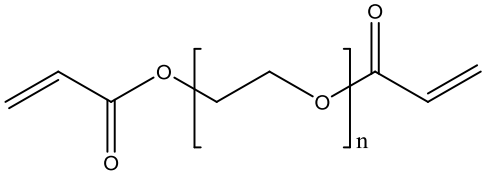

Figure 2.3. PEGDA [poly(ethylene glycol) diacrylate

2.1.2.2. Applications of PEG Hydrogels

2.1.2.2.1. Homogenous PEG Hydrogels

In order to treat various types of diseases such as diabetes, hypoparathyoidism, cancer, Parkinson's and Huntington's disease [36, 46] and to unravel characteristics of tissues, mimicking the natural environment and protection from immune system are significant. Natural environment provides different levels of stiffness, porosity, topology and morphogens for each tissue. By specifically mimicking desired tissue, tissue regeneration/development and elimination of requirement for donors will be achieved. Even at the cellular level, processes such as migration, differentiation, proliferation and apoptosis need to be investigated for tissue engineering. Also, controlled release of biological active components can be performed.[5] For this, PEG hydrogels are engineered with soluble/immobilized growth factors, proteolytically degradable sequences or adhesion peptides in studies such as vascularization, immunoprotection of pancreatic islets, chondrocyte metabolism, fibroblast migration and proliferation, human mesencymal stem cell viability.[12-14, 47, 48]

For these studies to be applicable *in vivo*, in addition to biocompatibility and mechanical stability, membrane permselectivity should be characterized. Hydrogel membrane should allow for the transfer of oxygen, nutrients, metabolites, wastes and when required, transfer of therapeutic agents, but it should be resistant to immune system components. As a result, balance between mass transport and molecular weight-cut-off for material has a strong effect on encapsulated cell viability and functionality.[36]

Key determinants of permeability for PEG hydrogels are backbone chemistry, crosslinking density, swelling ratio, molecular weight and concentration.[36] As a result, characterization of the membrane is as crucial as its functionality for supporting cells in tissue engineering applications. For example, Bryant et al. encapsulated chondrocytes in

PEG hydrogels for development of articular cartilage and reported that increasing crosslink density and mesh size caused higher decrease in cell proliferation and viability, as crosslinking density has effect on swelling ratio, and mesh size. These two parameters determine the amount of water uptake, molecular weight cut-off and solute diffusion rate through the hydrogel.[47] Additionally, Lin and her colleagues showed that chondrocyte behavior was affected heavily by mesh size: large mesh size supports chondrocyte viability and more collagen deposition, less glycosaminoglycan synthesis. [49] In another study, Moon et al. showed that increase in swelling ratio supported more branch formation by HUVECs in angiogenesis. When these hydrogels were transplanted into mouse cornea, invasion of blood vessel through VEGF including hydrogel and inosculation were clear.[12] In another study, Bott et al. showed that human dermal fibroblasts had higher proliferation rate in stiffer MMP sensitive PEG hydrogels.[15] Similarly, vocal fold fibroblast showed higher proliferation rate and lower ECM protein deposition in higher mesh size (lower elastic modulus).[50] Also, cell clusters such as pancreatic islets were covered with PEG hydrogel membrane to protect the cells from immune attack. Weber et al. showed that this procedure did not interfere with islet function and viability. Although islets showed similar viability with networks of higher molecular weights of PEG that present larger pores provided faster and more insulin release.[51]

In addition to cell and cell based drug delivery studies, PEG incorporated hydrogels function as carriers to release various proteins and growth factors including bovine serum albumin, vitamin B12, ovalbumin, lysozyme, immunoglobulin G, insulin, myoglobin, and the vascular endothelial growth factor.[8, 9, 11, 51] In these applications, capability to release specific molecular weight is a good indicator to determine molecular weight cut-off membrane, since in addition to their therapeutic activity, they provide clues about upper limit of the membrane.[36] Moreover, side effects of bolus injection can be

overcome, half life of the agent can be prolonged and site specific controlled delivery can be done with hydrogels, since oral or transdermal administration decreases bioactive molecule bioavailability due to denaturation and degradation. Also, these molecules readily have short half-life, usually less than one hour. For example, after intravenous injection, VEGF has half life of ~50 min and high burst concentrations can cause severe problems such as embryonic lethality and malformed vessel induction.[11, 52, 53] For this reason, it would be important to characterize the diffusivityof those molecules. In addition to physical entrapment, growth factor can be covalently incorporated into the PEG hydrogel network. For example, Zisch and his colleagues used physically entrapped and covalently immobilized VEGF in proteolytically degradable PEG hydrogels in rats. The results showed that both methods support vasculogenesis and covalent immobilization protects active conformation of the protein. They also concluded that growth factor was kept from inactivation by proteases and immediate clearance.[11]

2.1.2.2.2. Gradient PEG Hydrogels

In their natural environment, cells experience various types of gradients ranging from soluble growth factor to stiffness gradients. These gradients direct cells to specific fate including differentiation, migration and proliferation. During the last few years, researchers investigated the possibility of mimicking extracellular matrix in order to get detailed information at the cellular level.[5] As a result of its desirable properties (in Section 2.1.2.1) PEG hydrogels are accepted as one of the possible candidates to produce gradients to study cell behavior *in vitro* and to study sustained protein release. The remarkable examples are explained below and in all cases; gradient hydrogels are produced in a two step approach: gradient formation followed by stabilization by crosslinking.

2.1.2.2.2.1. Chemical Gradients in PEG Hydrogels

Chemical gradients in PEG hydrogels are applied to control cell behavior by covalent or physical incorporation of soluble growth factors and adhesion sequences.In 2005, DeLong et al. produced gradients of covalently immobilized bFGF on PEG hydrogels with a gradient maker to get detailed insights about cell migration and proliferation during tissue regeneration. By using human aortic smooth muscle cells as models, they showed that bFGF induced more proliferation compared to hydrogels without bFGF. Further, the experiments showed that cells migrated towards increasing concentrations of bFGF. They concluded that these gradients hydrogels can be applicable for effect of protein gradients on cell behavior.[54] At the same year, they also showed that immobilized gradients of RGDS are useful to study migration behavior human dermal fibroblasts. As expected, these cells migrated towards higher concentrations of RGDS.[54]

In another study, Peret and Murphy applied PLGA microspheres in PEG hydrogels. They simply encapsulated BSA in microspheres. In the following step, they incorporated these spheres in prepolymer solution and after settling down, they formed the hydrogel by photo-crosslinking. The result was soluble protein concentration gradients in the hydrogel. They concluded that soluble protein gradients in natural cell environment can be mimicked by this way to study tissue development and regeneration as well as controlled release.[55]

2.1.2.2.2.2. Physical Gradients in PEG Hydrogels

Changes in physical properties such as porosity and stiffness are another prominent class of environmental factors for regulating diffusion and cell behavior. For this purpose,

Chatterjee et al. produced PEG hydrogels with porosity (permeability) and stiffness gradients. These gradients are used to study osteoblast behavior, since modulus gradients are required for successful development of mineralized tissues and to support tissue regeneration. They observed that increased modulus resulted in enhanced cell viability in softer segments, since these regions swell more and as a result, they facilitate molecule transport. In contrast, increasing modulus (increasing stiffness, decreasing porosity) induced osteoblast differentiation and mineralization.[56]

In order to address the importance of bioinertness and cellular behavior response to mechanical gradients, Nemir and West applied patterned elasticity on PEG hydrogels, and illustrated the effect of rigidity of macrophage adhesion. The results indicated that increasing rigidity (stiffness) promotes more macrophage adhesion to the substrate surface. They also generated porosity gradients in PEG hydrogels with the use of a gradient maker, and characterized mechanical properties. The results demonstrated that softer surfaces had lower elastic modulus with higher water content.[17]

In addition to these studies, Cruise et al. used PEG hydrogel formed by surface initiated (interfacial) photopolymerization to characterize permeability structure. [8] This method allowed them to produce permeability gradients in a single step. They formed hydrogels from 2-20 kDa PEGDA with concentrations ranging from 10% to 30% and they were able to prove that this micrometer thick can limit the diffusion of molecules with molecular weights higher than ~17 kDa.[8] During the same year, the authors used interfacial photopolymerization to optimized conditions, and synthesized uniform layers around pancreatic islet in order to protect them from immune system and to support both viability and functionality.[57] In 2004 and 2006, Kızılel and her colleagues used surface initiated photopolymerization on glass surfaces, where photoinitiator was covalently bonded to the underlying substrate. Hydrogels synthesized with this approach could be

formed in multilayers with or without patterns, which can be utilized to generate permeability gradients, or to localize proteins with gradients in multilayers. [6, 23]

All of these previous studies demonstrated that, by regulating network properties such as pore size and pore size distribution (porosity gradient), it is possible to determine cell behavior and controlled release of bioactive molecules from gradient PEG hydrogel networks. In this study, the regulation of mesh size distribution was controlled by the molecular weight and concentration of PEGDA monomer in PEG based hydrogel prepolymer solution. Physical characterization with swelling experiments and release of protein/peptide showed that these hydrogels with gradients have mesh sizes large enough for the diffusion of GLP1 (9-37) peptide, and for larger proteins such as BSA. The diffusion results for BSA and GLP1 (9-37) showed that hydrogels synthesized with this approach are applicable for controlled delivery of bioactive molecules.

Bovine serum albumin (BSA) is a water soluble monomeric protein with 66.4 kDa molecular weight consisting of 583 amino acid residues in a single chain. This class is important for the transfer of insoluble fatty acids in the body through circulatory system. It also functions in regulation of blood pH. Its multifunctional properties results from its affinity for many ligands and as a result, it is one of the crucial molecules for transfer and deposition of a broad range of molecules in therapeutic experiments. Other advantages are low cost, wide availability, structural and functional similarity to human serum albumin (HSA).[58-60] Further, diffusion studies were carried out with BSA, a model widely applied protein for various natural and/or synthetic degradable/nondegradable scaffolds including proteolytically degradable PEG hydrogel, hyaluronic acid-poly(ethylene) glycol hydrogels, pegylated PLGA nanoparticles, PVA networks, poly(orthoester) extruded thin strands, alginate hydrogels, PEG-poly(N-isopropylacrylamide) hydrogels, chitosan nanoparticles, PEO and PEG hydrogels. [61-70]

Glucagon-like peptide 1 (GLP1) is an incretin hormone released from L cells in the intestine after meal ingestion. It acts on insulin biosynthesis, protects β-cells by decreasing apoptosis and increasing proliferation. It negatively regulates glucagon secretion. Insulinotropic component is GLP1 (7-37) fragment and when it is secreted, dipeptidyl peptidase-4 (DPP-4) cleaves first two amino acid residues from the N-terminus (histidine and alanine) resulting GLP1 (9-37) fragment. This peptide has a random coil structure and is known as noninsulinotropic and biologically inactive.[71] GLP1 (7-37) has application for therapeutic studies. For example, Kızılel and her colleagues formed GLP1 (7-37) biofunctionalized PEG using a layer-by-layer assembly technique for rat pancreatic islet encapsulation and delivery. They concluded that individually coated islets showed enhanced insulin secretion and viability compared to naked islets.[72] Also, Kızılel showed theoretical modeling of GLP in PEG hydrogels formed by surface initiated photopolymerization. This model provided information about crosslink density, swelling, thickness of the hydrogel and showed how gradient of covalently immobilized GLP can be achieved.[19] Although GLP1 (9-37) applied in such studies, diffusivity properties of the peptide has not been reported..

Encapsulation of NIH 3T3 fibroblasts within RGDS functionalized PEG hydrogel showed that PEG hydrogels with permeability gradients possess the property of permeability. The reason for RGDS to be chosen as adhesion peptide for fibroblasts is that this fibronectin derived tetrapeptide supports and stimulates fibroblasts for various cellular processes including adhesion, attachment, migration, proliferation and extension. This functionality is achieved by interactions between RGDS and integrins such as $\alpha_5\beta_3$ and $\alpha_V\beta_3$ located on cell surface. Similar interactions were also found for cells such as smooth muscle, osteoblast, endothelial and neural cells. [32, 73-75]

2.1.2.3. General Mechanisms of PEG Hydrogel Formation

PEG based hydrogels can be synthesized by chemical crosslinking, ionic and physical interactions. In many studies, physically or covalently crosslinked hydrogels are being studied to obtain hydrogel structures. Depending on the reaction mechanism, chemically crosslinked PEG hydrogels are classified into three groups: Chain growth, step growth and mixed mode mechanism. [76] (Figure 2.4)

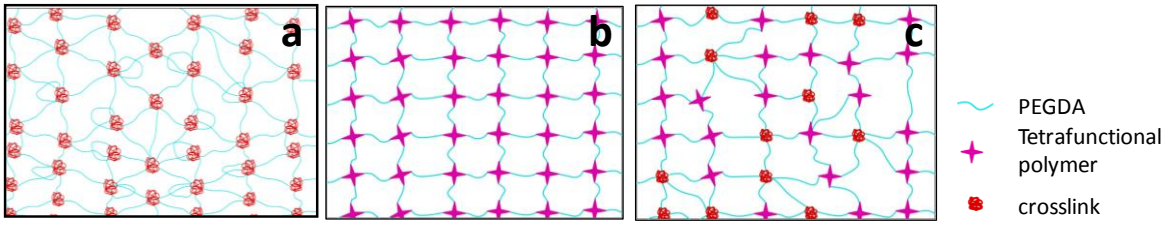

Figure 2.4. Networks structures from mechanism of a) chain growth, b) step growth, c) mixed mode

In chain growth polymerization (Figure 2.4a), propagation occurs through centers presenting carbon-carbon double bonds. Completion of reaction leads to formation of covalently crosslinked high molecular weight polymer chains. During reaction, radical species are generated by thermal energy, redox reactions or excitation of photoinitiator with UV (ultraviolet) or visible light. Among these chain growth reactions, photopolymerization is the most commonly used mechanism applied for hydrogel formation.[76] The free radical polymerization (photopolymerization) scheme in covalent crosslinking is divided into three parts:

1. Initiation (formation of radical species from nonradicals)
2. Propagation (radical transfer to a substituted alkene)

3. Termination by disproportionation and combination (atom transfer and atom abstraction reactions and radical–radical recombination reactions) [77]

This mechanism can be used at short irradiation times and mild conditions, where hydrogel structures would form at room or physiological temperatures with little heat generation. It provides spatial and temporal control and can be used to make hydrogels *in situ* with laparascopic devices or catheters with minimal invasiveness. For this application, subcutaneous injection is followed by transdermal illumination, which leads to the formation of hydrogel. Disadvantages may arise due to the oxygen acting as a scavenger and incomplete double bond conversion. These problems are overcome by triggering reaction under inert gas, adjusting initiator concentration and type or using accelerators.[78, 79]

In contrast, in step growth polymerization (Figure 2.4b), multifunctional monomers react to make hydrogel network. In this mechanism, the required monomer functionality is equal or greater than two.[41] One way for step growth reaction is the Michael type addition reaction, which was developed by Hubbell and his colleagues. The mechanism includes reaction between multifunctional PEG (eg. acrylate, maleimide and vinyl sulfone) and dithiols under physiological temperature and pH.[39] The major drawbacks of this reaction scheme are possible reaction with the cytosine residues of proteins, long polymerization time and lack of control in the network structure. Protein interaction causes reduced bioactivity and denaturation leading to a severe immune response.[41] Click chemistry is another step growth polymerization technique applied to form PEG based networks. In this chemistry, azide and alkyne groups of macromers are reacted in the presence of catalysts. Although this mechanism forms hydrogels with superior mechanical properties and controlled structure, the major catalysts, copper ions, are problematic for cell encapsulation.[41]

In mixed mode gelation, thiol acrylate photopolymerization occurs. The resulting network structure is represented in Figure 2.4c. It includes properties from chain growth and step growth reactions. During reaction, growing polymer chains transfer chains to thiol monomers.[41]

2.1.2.4. Formation of PEG Hydrogels

In this thesis, PEG hydrogels are formed by surface initiated photopolymerization. This class of photopolymerization is a type of chain growth polymerization and creates permeability gradients beginning from the prepolymer and underlying surface interface. Protein release through these hydrogels was studied, and cytocompatibility experiments were performed with these hydrogels.

Bovine serum albumin is used for the physical adsorption of of photoinitiator, eosin Y, onto the surface of polystyrene dishes. Eosin Y is chosen as an initiator, since its spectral properties fits for an argon ion laser. Precursor solution for hydrogel includes triethanolamine (TEA), 1-vinyl-2-pyrrolidinone (NVP) and PEGDA (Figure 2.5).[6]

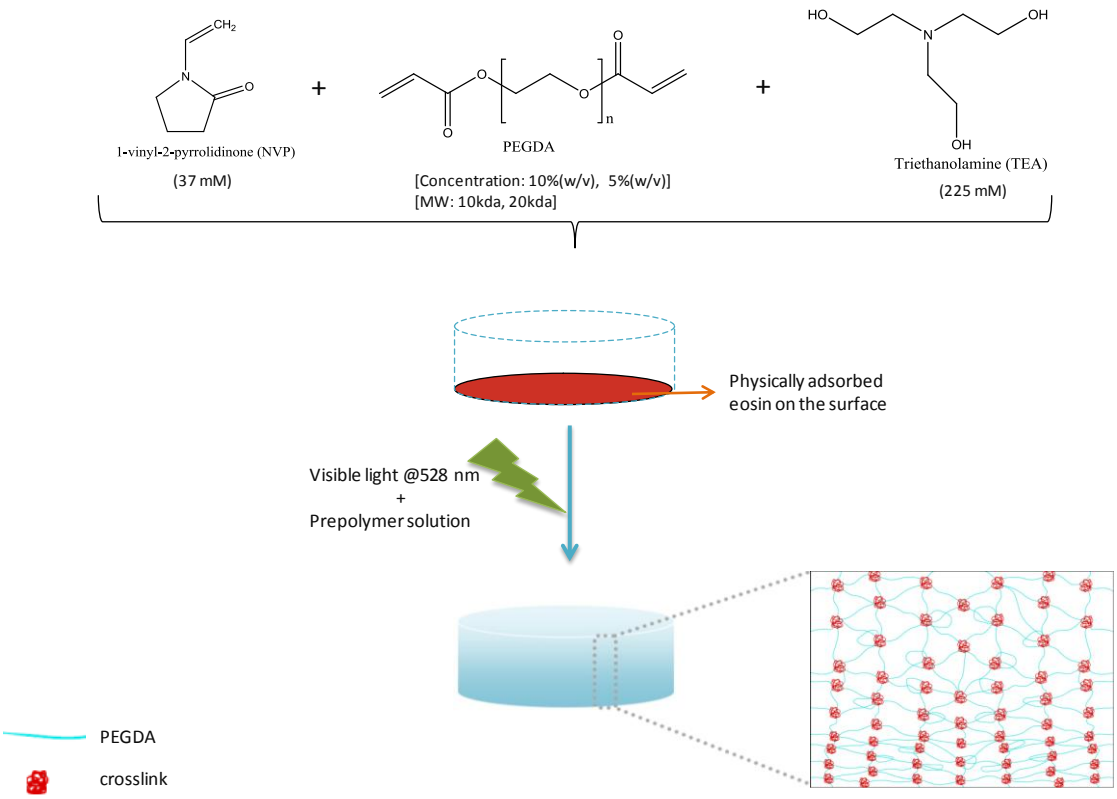

Figure 2.5. Schematic representation of PEG hydrogel formation

When a pre-polymer solution is placed on top of the initiator immobilized surface and exposed to green light, eosin Y on the surface creates the initial radical in the presence of electron donor, TEA acting as co-initiator. In this mechanism, TEA transfers electron to eosin Y. In turn, dye in the triplet state forms an eosin anion radical and a TEA cation radical. The reaction is followed by immediate proton loss from TEA generating a neutral TEA. Proton lost from TEA converts eosin anion radical to neutral eosin Y (Figure 2.6). Alpha-amino radical from TEA is the main radical to initiate photopolymerization.[6]

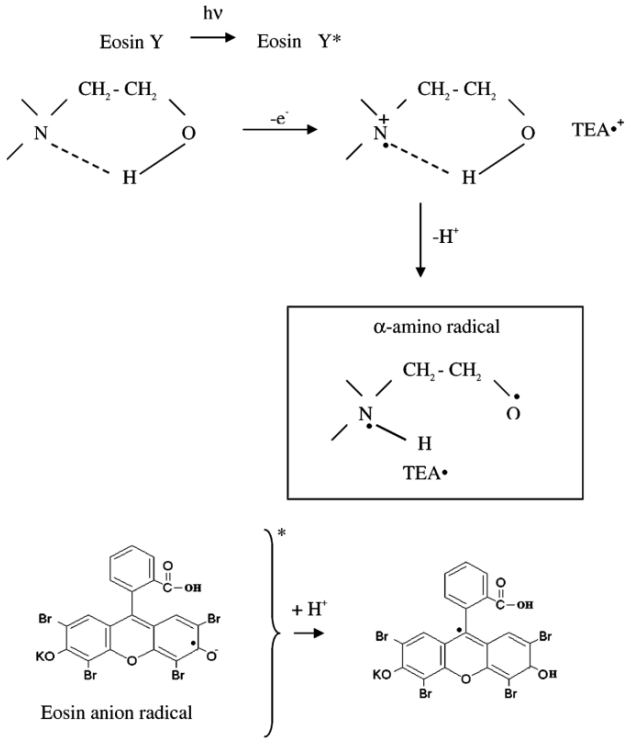

Figure 2.6. Initiation reaction mechanism of PEG hydrogel [6]

Radical reaction continues through pendant double bonds (PDB) on PEGDA. Crosslinking followed by combination causes termination. Live radicals propagate through PEGDA. A live radical can interact with another live radical or PDB of a dead monomer. The result is either a branched dead polymer or a new live radical. At the end of the reaction, the interaction of two live radicals forms a quaternary branch point or crosslink (Figure 2.7).[19, 80] NVP in the system acts as an accelerator to increase polymerization rate and to decrease the number of uncrosslinked polymer chains.[79]

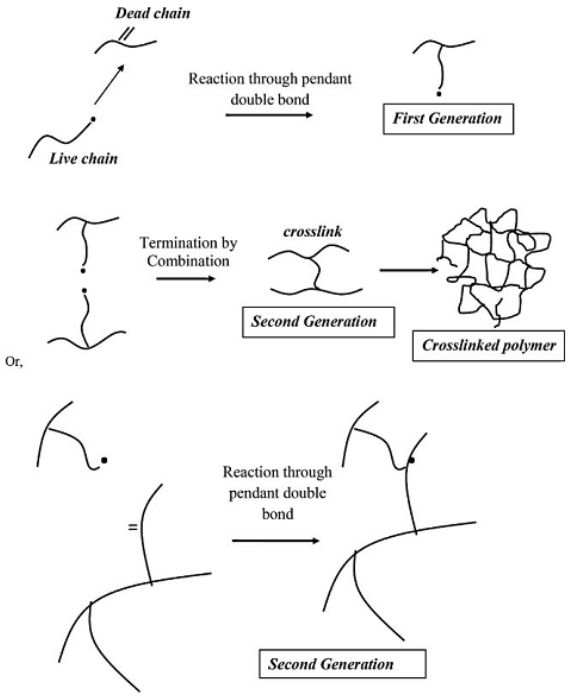

2.7. Steps in PEG hydrogels formation with PEGDA/NVP copolymerization [80]

Chapter 3

EXPERIMENTAL PART

3.1. Materials

10 kDa and 20 kDa poly(ethylene glycol) diacrylate (PEGDA) was purchased from, Laysan Bio, Inc. 1-vinly-2-pyrrolidinone (NVP) and triethanolamine (TEA) were obtained from Aldrich and Merck, respectively. Sodium bicarbonate ($NaHCO_3$) was obtained from Merck. Phosphate buffered saline (PBS) was purchased from Amresco. Eosin Y was purchased from Sigma Aldrich. Acrylate-PEG-N-hydroxysuccinimide (acrylate-PEG-NHS) was obtained from Nektar Transforming Therapeutics. Arg-Gly-Asp-Ser (RGDS) and glucagon like peptide 1(9-37) (GLP1 (9-37)) were purchased from Elim Biopharmaceuticals, Inc. Dulbecco's Modified Eagle Medium (DMEM) and fetal bovine serum (FBS, heat inactivated) were obtained from Gibco. L-glutamine (200 mM), penicillin-streptomycin, (stabilized, 10,000 units penicillin and 10 mg streptomycin/mL, penn-strep) and trypsin-EDTA (25%) were purchased from Sigma. BSA was purchased from SantaCruz. The CellTiter-Glo Luminescent Cell Viability Assay was obtained from Promega and slide-a-lyzer dialysis cassettes (MWCO 3500) were purchased from ThermoScientific. 24 well plates and tissue culture dishes were purchased from Greiner Bio-one.

3.2. Methods

3.2.1. Swelling Experiments

3.2.1.1. Synthesis of PEG Hydrogels for Characterization

Prepolymer solutions were prepared with concentrations between 2% and 15% (w/v) PEGDA (10 or 20 kDa), 225 mM TEA and 37 mM NVP in 10 mM PBS at pH 8. Eight mm diameter surfaces were functionalized with 1 mg/ml BSA for 30 min at dark at room temperature. To remove excess unbound BSA, surfaces were washed two times with 10 mM PBS. Following 30 min, surfaces were incubated with 10 mM eosin Y at dark at room temperature. This process allowed eosin Y to physically attach to the surface. At the end of eosin Y incubation, surfaces were rinsed with 10 mM PBS once. Prepolymer solution was placed on top of these surfaces and exposed to argon ion laser (2.5 mW/cm^2, 10 min, Coherent Inc., Santa Clara, CA). After photopolymerization, synthesized PEG hydrogels were placed in 10 mM PBS (pH 7.4) and incubated at 37°C. At specific time points, wet weights were measured. After reaching equilibrium, hydrogels were freeze dried and dry weights were measured. These wet and dry weights were used to calculate mass swelling ratio, molecular weight between crosslinks and mesh size.

3.2.1.2. Calculation of Hydrogel Network Parameters: Swelling ratio, M_c and Mesh Size

After measurement of wet and dry weight, mass swelling ratio, q, was calculated with equation 3.1.

$$q = \frac{W_s}{W_d} \tag{3.1}$$

Here, W_s and W_d represent weight at swollen (wet) and dry states, respectively.[81] Volumetric swelling ratio, Q, was calculated as:[79]

$$Q = \frac{V_s}{V_d} = 1 + \frac{\rho_p}{\rho_s}(q-1) \tag{3.2}$$

where, ρ_s and ρ_p are densities of the solvent (water,1 g/cm^3) and polymer (PEG, 1.12 g/cm^3), respectively. V_s is the volume in the equilibrium swollen state and V_d is the dry polymer volume.

Molecular weight between crosslinks was calculated with Peppas-Merrill equation (Equation 3.3) derived from Flory-Rehner equation. This equation is frequently applied for neutral polymers and assumes the presence of solvent during the polymerization.[81]

$$\frac{1}{M_c} = \frac{2}{M_n} - \frac{\left(\frac{\overline{\upsilon}}{V_1}\right)\left(\ln(1-\nu_{2,s}) + \nu_{2,s} + \chi\nu_{2,s}^2\right)}{\nu_{2,r}\left[\left(\frac{\nu_{2,s}}{\nu_{2,r}}\right)^{1/3} - \left(\frac{\nu_{2,s}}{2\nu_{2,r}}\right)\right]} \tag{3.3}$$

$$\overline{\upsilon} = \frac{1}{\rho_p} \tag{3.4}$$

M_c and M_n are the molecular weight between crosslinks and chain length of the starting polymer, respectively. V_1 is the molar volume of the solvent (water, 18 cm^3/g), χ

is Flory-Huggins interaction parameter (0.426). $\bar{v}$ is the specific volume of the polymer and calculated using equation 3.4. In this equation, ρ_p is density of the solvent (water, 1 g/cm^3) and polymer (PEG, 1.12 g/cm^3). $v_{2,r}$ and $v_{2,s}$ are polymer volume fraction of the hydrogel in the relaxed (after preparation) and swollen state, respectively.[8, 9, 81, 82] These volume fractions were calculated with equations 3.5 and 3.6.

$$v_{2,r} = \frac{v_d}{v_O} \tag{3.5}$$

$$v_{2,s} = \frac{v_d}{v_s} = \frac{1}{Q} \tag{3.6}$$

V_d is the volume of the dry polymer sample, V_o is the gel sample volume before equilibrium swelling and V_s is the gel sample volume after equilibrium swelling.[83]

M_c values were used to calculate root mean squared end-to-end distance of the unperturbed (solvent-free) state and mesh size with Canal-Peppas equations.

$$(r_O^{-2})^{1/2} = 1\left(2\frac{M_c}{M_r}\right)^{1/2} C_n^{1/2} \tag{3.7}$$

$$\xi = (r_O^{-2})^{1/2} v_{2,s}^{-1/3} \tag{3.8}$$

where $(r_o^{-2})^{1/2}$ is the root mean squared end-to-end distance of the unperturbed (solvent-free) state, l is the bond length (1.50 Å), M_r is the molecular weight of PEG

repeat unit (44 g mol^{-1}), C_n is the characteristic ratio for PEG (4) and ξ is mesh size (Å). [8, 84]

3.2.2. Diffusion Experiments

3.2.2.1. Synthesis of PEG Hydrogels for Protein Release

For this study, bovine serum albumin (BSA) and glucagon like peptide 1 (9-37) (EGTFTSDVSSYLEGQAAKEFIAWLVKGRG) (Table 3.1) were chosen as biological molecules for release studies. In the following table, diffusivities in water were calculated with Stokes-Einstein equation (equation 3.9) assuming that diffusion occurs in a dilute medium and solute molecules having nearly spherical structures are larger than solvent molecules.[85, 86]

$$D_O = \frac{kT}{6\pi\eta R_s} \tag{3.9}$$

In this equation, D_0 is diffusivity in water at a given temperature, η is viscosity of water (6.915×10^{-4} Nm/s^2), R_s solute radius, k is Boltzman's constant (1.38×10^{-23} J/K), T is temperature (310 K).[51]

Table 3.1. Released protein/peptide properties

Protein	Molecular weight (Da)	Diffusivity at 37°C in water ($\times 10^{-6}$ cm^2/s)	Hydrodynamic radius (nm)
BSA	66,400	0.92	3.56[51]
GLP1(9-37)	3148	2.52	1.3[87]

PEGDA prepolymer solutions were prepared as in Section 3.2.1.1 with incorporation of protein/peptide at a final concentration of 1.5-2% (w/v) (Figure 3.1). After photopolymerization, each hydrogel was placed into 5 ml PBS and incubated at 37°C. At specified time points, 0.2 ml sample was removed and replaced with fresh PBS. Protein content of the samples was measured at 280 nm (ThermoScientific Nanodrop 1000 Spectrophotometer).

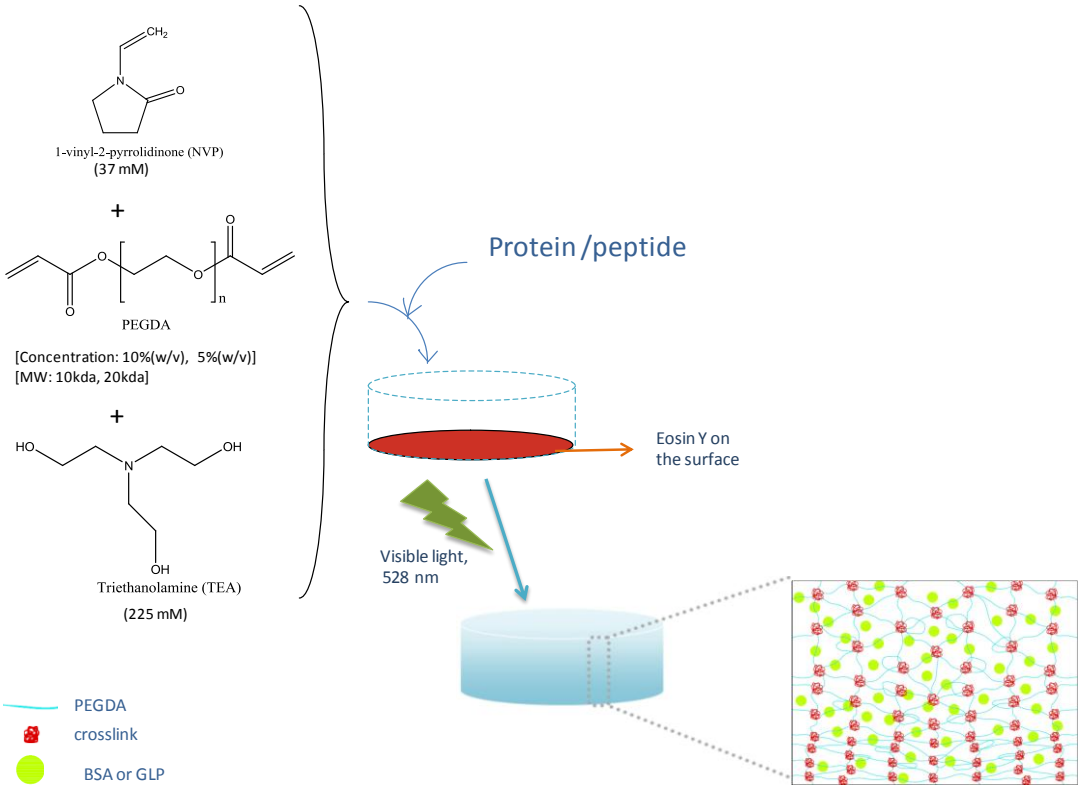

Figure 3.1. Scheme of formation of PEG hydrogels for protein release studies

3.2.2.2. Release Profiles of BSA and GLP1 (9-37)

For the analysis of protein content, mass balance was performed (equation 3.10).[9]

$$M_i = C_i V + \sum C_{i-1} V_s \tag{3.10}$$

where M_i is mass released at time i (mg), C_i is the concentration of solute at time i (mg/ml), V is the volume of the solution (5 ml) and V_s is the sample volume.

Calculated M_i values were normalized with initial protein mass (M_{inf}) and release profiles were obtained.[9]

3.2.2.3. Calculation of Effective Diffusion Coefficients

For effective diffusion coefficients, modified Fick's law derived by Korsmeyer-Peppas was used as follows:[9, 88, 89]

$$\frac{M_i}{M_{\inf}} \cong 4\left[\frac{D_e t}{\pi \delta^2}\right]^{1/2} \tag{3.11}$$

where M_i and M_{inf} is mass released at time i (mg) and initial protein mass (mg), respectively. D_e represents effective diffusion coefficient, t is time (min) and δ is the hydrogel thickness (cm). This equation shows that profile of M_i/M_{inf} vs. $t^{1/2}$ gives effective diffusivity in the region of $M_i/M_{inf}<0.6$.

This equation assumes that one dimensional diffusion occurs with negligible side effects through an insoluble matrix in the infinite medium and is valid for short release times. The solute concentration within the matrix should be lower than the solubility of the molecule. It is widely applied in monolithic systems when the release mechanism is unknown.[62, 89, 90]

3.2.3. Cytocompatibility of PEG Hydrogels

3.2.3.1. Synthesis of Acrylate-PEG-RGDS

Conjugation was performed by reacting acrylate-PEG-NHS with RGDS in 1:1 molar ratio in 50 mM $NaHCO_3$ buffer (pH 8.2) for 2 h while shaking at 100 rpm at room temperature at dark (Figure 3.2). The product was dialysed to remove unreacted peptide and acr-PEG-NHS.[12, 43]

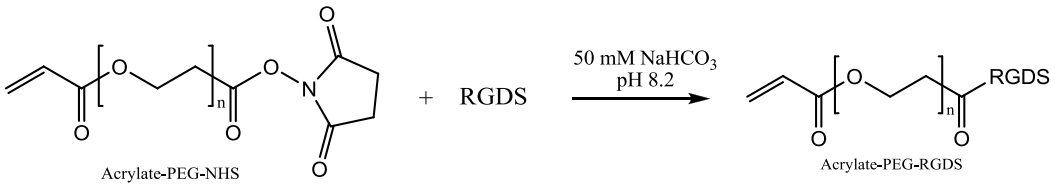

Figure 3.2. Synthesis scheme for acr-PEG-RGDS.

3.2.3.2. Culture of NIH 3T3 Fibroblasts

NIH 3T3 fibroblasts were maintained in DMEM supplemented with 10% FBS, 2 mM L-glutamine, 1000 U/ml penicillin and 100 mg/ml streptomycin. They were grown passages between 4-12. Cells were maintained in a humidified environment at 37°C with 5% CO_2.

3.2.3.3. Encapsulation of NIH 3T3 Fibroblasts

Eosin Y attached surfaces were prepared as mentioned above. Prepolymer solutions were prepared with 5% and 10%(w/v) PEGDA (10 or 20kDa), 225 mM TEA and 37 mM NVP in 10 mM phosphate buffered saline (PBS) at pH 8. Immediately before photopolymerization, acr-PEG-RGDS (RGDS concentration as 2 mM) and fibroblasts

($1x10^6$ cells/ml) were added to 50 µl prepolymer solution. Prepolymers on eosin Y attached surfaces were exposed to argon ion laser at 2.5 mW/cm^2 for 10 min (Figure 3.3). Resulting hydrogels were placed into 24 well plates (Greiner Bio-one) and fed with 750 µl cell culture medium used for maintenance of fibroblasts. Medium was refreshed every other day.

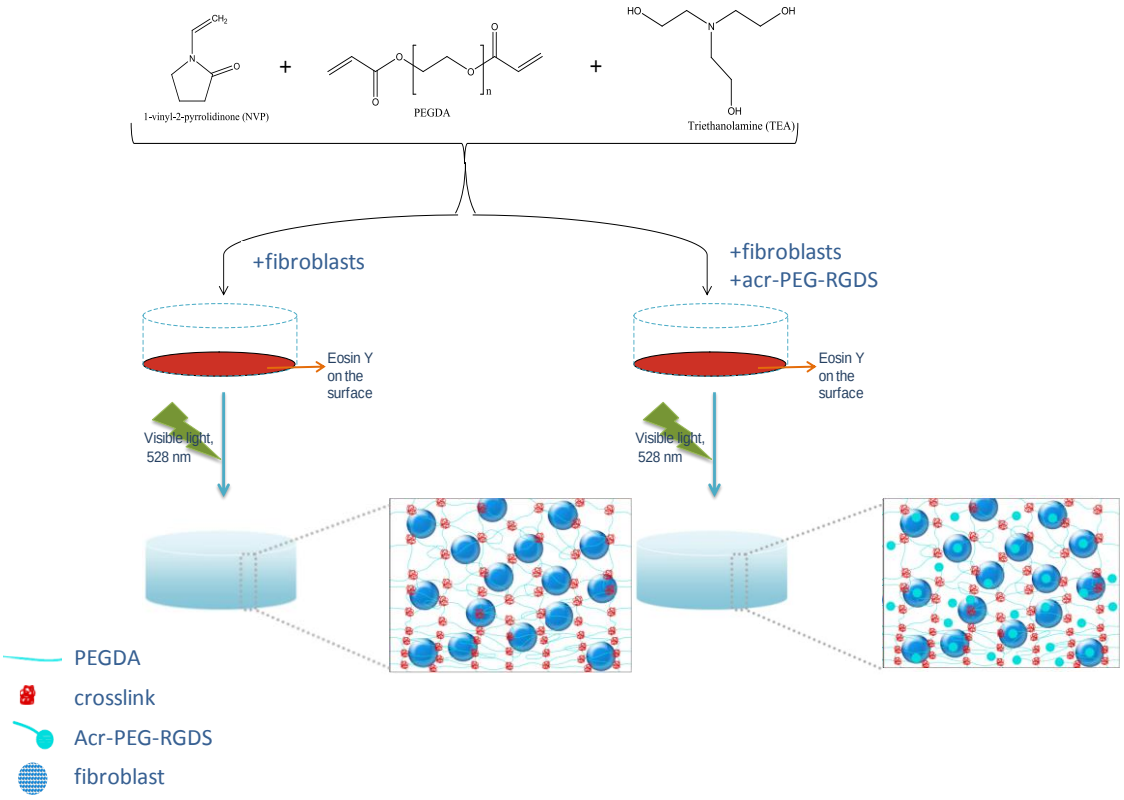

Figure 3.3. Encapsulation of fibroblast within PEG hydrogels

3.2.3.4. Viability

The CellTiter-Glo Luminescent Cell Viability Assay was performed for day 1 and 3 to measure intracellular ATP content. Briefly, encapsulated cells were incubated in 50% CellTiter-Glo reagent at 100 rpm for 1h. After incubation, 200 µl from each sample was

removed and luminescence was measured with a luminometer (Thermo Electron Cooperation, Fluoroskan Ascent FL).

3.3. Statistical Analysis

All data sets are analyzed using one-way analysis of variance (ANOVA). The results were represented as the mean value (±SD) of at least triplicate samples. P-values less than 0.05 were considered statistically significant.

Chapter 4

RESULTS AND DISCUSSION

4.1. Physical Characterization

4.1.1. Effects of Concentration and Molecular Weight of PEGDA on Equilibrium Mass and Volumetric Swelling Ratios

In tissue engineering applications, one of the main goals is the production of a semipermeable membrane that prevents of immune rejection while providing transportation of nutrients, wastes, therapeutic agents, oxygen and carbon dioxide. For this purpose, it is crucial to determine how much water uptake occurs, since this property depends on membrane pore size. It also gives information about water content which should be high enough to support both cell viability and functionality as in ECM and if achieved, it should be able to mimic gradient structure that can be used to create soft tissues *in vitro*. It can also give information about native behavior of cells in healthy or diseased state. This hydrophilicity is also important to release hydrophilic drugs or growth factors from PEG based networks for controlled release.[36, 41]

Since water-sorption property is an indicator of hydrophilicity [21], to understand nanoscopic properties, first step was swelling experiments for determination of water content. In this study, permeability gradients were produced by surface initiated photopolymerization under mild, physiological conditions by copolymerization of PEGDA and NVP in a single step.

For swelling studies, molecular weight of 10 kDa and 20 kDa PEGDA between

concentrations of 2 and 10% concentration were used to determine the effect of molecular weight and concentration of PEGDA on equilibrium swelling ratio. For 20 kDa and 10 kDa PEG hydrogels, increasing concentration from 2 to 15% decreased both mass and volumetric swelling ratio significantly (Figure 4.1 and Table 4.1). The mass swelling ratio was reduced from ~29 to ~19 and volumetric swelling ratio was ranged from ~32 to ~21 for 20 kDa PEG hydrogel within the PEGDA concentration range of 2-15%. For 10 kDa hydrogels, mass swelling ratios in the equilibrium were ranging from ~32 to ~15 for 2% and 15% PEG. For these conditions, volumetric swelling ratio was ~36 and ~15 for 2% and 15% PEG hydrogels, respectively.

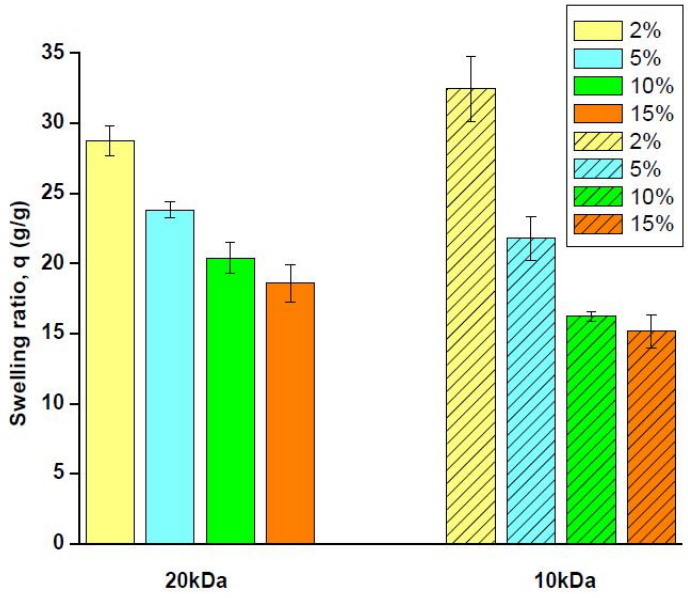

Figure 4.1. Effect of PEGDA molecular weight and concentration on mass swelling ratios of PEG hydrogels. The group means of 20 kDa significantly differ from each other, but no statistically significant difference was observed between 20 kDa, 10% and 15%. Similarly, the group means of 10 kDa significantly differ from each other, but no statistically significant difference was observed between 10 kDa, 10% and 15%.

Table 4.1. Properties of PEG hydrogels synthesized in this study.

M_n(g/mol)	% PEGDA (w/v)	Volumetric swelling ratio, *Q*	Crosslinkable double bonds (mol/l)
10 000	2	36.21±2.60	0.004
10 000	5	24.28±1.74	0.01
10 000	10	18.06±0.37	0.02
10 000	15	15.15±1.34	0.03
20 000	2	32.07±1.20	0.002
20 000	5	26.55±0.66	0.005
20 000	10	22.72±1.24	0.01
20 000	15	20.69±1.47	0.02

The results showed that at constant molecular weight, decrease in concentration is inversely related to mass and volumetric swelling ratio whereas at constant concentration, mass and volumetric swelling ratios were proportional to molecular weight. This is because, increase in concentration or decrease in molecular weight forms denser networks with higher crosslink density. The tighter network will have more chain entanglements and such network limitations prevent swelling.[51, 67] In a similar study, Cruise et al. used PEG hydrogels applying the similar technique used in this study, observed the similar trends for swelling ratio for PEGDA molecular weights ranging from 2 to 20 kDa with PEGDA concentration of 10, 20 and 30%.[8] When compared with our results, our system formed looser networks with higher water content due to lower number of eosin Y molecules attached to the surface. For hydrolytically degradable PEG hydrogels, Zustiak et al. showed that at constant concentration mass welling ratio decreased with higher concentration of PEG.[91] In other hydrogel systems including PVA and polyacrylamide, increasing concentration reduced water content due to increased concentration of number of crosslinks provided by higher concentration of polymer in the network structure.[69, 92-94]

The resulting differences caused by molecular weight and concentration can be explained by changes in network structure and crosslinkable double bonds. In our case, increasing concentration or decreasing molecular weight of PEGDA increases the number of PEG molecules and crosslinkable double bonds. This leads to formation of higher numbers of free radicals resulting in higher crosslink density (Table 4.1). Also, network defects such as chain entanglements resulting from radicalic process lowers swelling ratio and prevents swelling due to formation of tighter networks with less intrachain crosslinking.[36, 67]

4.1.2. M_c Values for PEG Hydrogels Formed by Surface Initiated Photopolymerization

Number average molecular weight between crosslinks is one of the critical network parameters used to describe hydrogel structure and to calculate mesh size which represents molecular weight cut off for the membrane (Figure 4.2).

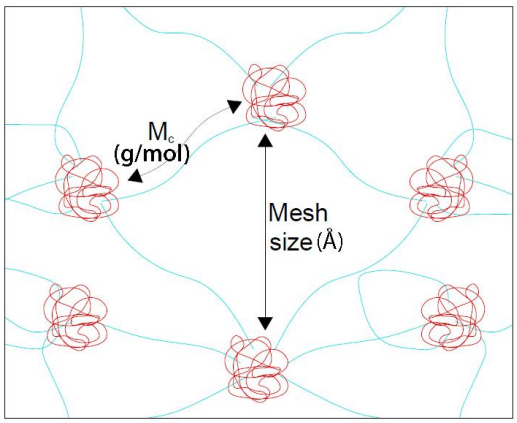

Figure 4.2. Network structure of PEG hydrogel

For this purpose, next step in this study was to determine M_c by using Peppas-Merrill equation along with the experimental swelling measurements.

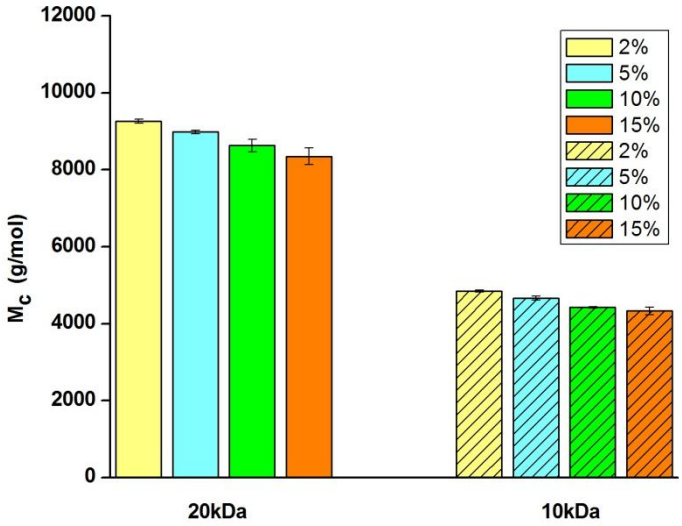

Figure 4.3. M_c for PEG hydrogels. The group means of 20 kDa significantly differ from each other, but no statistically significant difference was observed between 20 kDa, 2% and 5% as well as in between 10% and 15%. Similarly, the group means of 10 kDa significantly differ from each other, but no statistically significant difference was observed between 10 kDa, 10% and 15%.

As represented in Figure 4.3, M_c values were between ~9360 and ~8352 g/mol within the concentration range of 2% and 15% PEGDA for PEG hydrogels formed with 20 kDa molecular weight. Similarly, for PEG hydrogels formed with 10 kDa molecular weight, this parameter ranged between ~4849 and 4422 g/mol within the same concentration interval. Molecular weight between crosslinks was observed to be nearly independent of concentration for PEG chain, however it was influenced by molecular weight: Decrease of PEGDA molecular weight from 20 kDa to 10 kDa reduced M_c to the half of 20 kDa. Since at constant concentration, increasing molecular weight will cause incorporation of less number of PEG units, the network structure will be loose and as expected, the

molecular weight between such links will be larger in higher molecular weights due to longer chain length. At constant specific concentration, relation between molecular weight (ranging from 3.4 to 20 kDa) and M_c showed similar behavior as proved by Lin and colleagues.[49] At constant concentration or molecular weight, Cruise et al. also observed significant changes in M_c, increasing molecular weight or decreasing concentration significantly increased M_c .[8] These increases/decreases are reasonable, as increase in water content or PEGDA chain length lowers crosslink density resulting in higher M_c. [70, 95] Also, number average molecular weight between crosslinks should not be less than molecular weight of PEGDA, but in all cases, it was observed that these values were reduced. The probable causes are network defects such as chain entanglements as physical links arising from crosslinking.[96] Moreover, since at constant concentration, increasing molecular weight will cause incorporation of less number of PEG units, the network structure will be loose and as expected, the molecular weight between such links will be larger in higher molecular weights due to longer chain length. Similarly, at a specific molecular weight, decreasing concentration will show incorporation of less number of PEGDA molecules. This will form less number of free radicals and resulting hydrogels will be looser. Also, Burczak et al. observed such a trend for M_c in PVA hydrogels formed via photopolymerization and chemical crosslinking at constant concentration for swelling ratio and mesh size. Increased number of crosslinks due to higher monomer concentrations was also resulted in reduced values for M_c for other hydrogels formed with monomers other than PEGDA.[8, 92]

4.1.3. Effect of Molecular Weight and Concentration of PEGDA on Mesh Size

Mesh size is one of the key parameters used for determination of physical properties of hydrogels. Chemical structure of monomers, crosslinking density, external stimulus

including pH and temperature affect mesh size. It is a critical parameter for diffusion of molecules, since if solute has same size with mesh size, it will not be able to diffuse out theoretically. This parameter is also used to determine other physical properties such as diffusivity of releasing molecules, degradability and mechanical strength.[21, 92] For this purpose, next step in this study was to calculate mesh size from Canal-Peppas equations in section 3.2.1.2.

The mesh sizes were between 190 and 156 Å for 20 kDa PEG hydrogels within the concentration range of 2-15% whereas 10 kDa PEG hydrogels showed mesh size distribution between 143 and 105 Å in the same range (Figure 4.4).

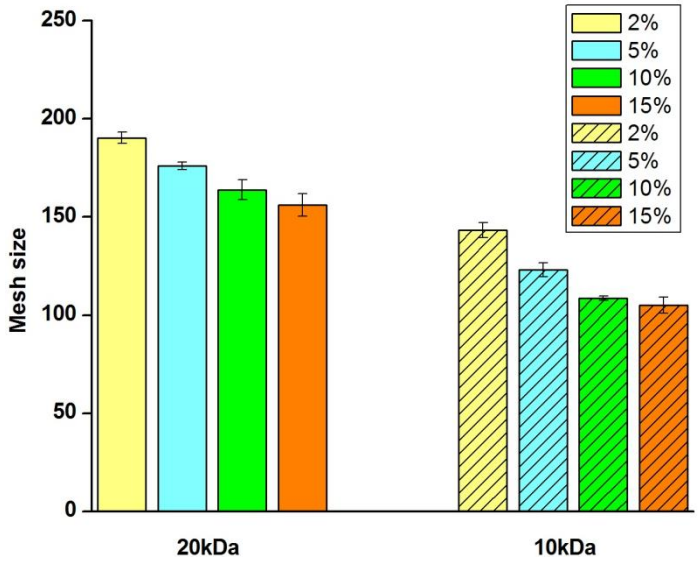

Figure 4.4. Mesh (pore) size (Å) distribution for PEG hydrogels. The group means of 20 kDa significantly differ from each other, but no statistically significant difference was observed between 20 kDa, 10% and 15%. Similarly, the group means of 10 kDa significantly differ from each other, but no statistically significant difference was observed between 10kDa, 10% and 15%.

Mesh size results showed similar trends with swelling ratio and M_c. The mesh size was inversely affected by concentration and increases at higher PEGDA molecular weight. Increases in PEGDA chain length and decreases in concentration induce increases in water content and reduce crosslink density.[95] As expected, hydrogels formed with higher molecular weight PEGDA monomers showed larger mesh size at constant concentration. Further, increases in concentration of PEGDA lead to decreases in mesh size. This is because, due to reduced crosslink density at higher M_c and swelling ratio, looser network structures will be observed and the resulting pores will be larger. This allows more water molecules transport and increases water content.[36, 92]

4.2. Diffusion Experiments

4.2.1. Release Profiles for BSA and GLP1 (9-37)

For drug/protein delivery applications, the requirement for prolonged site specific delivery is clear. To satisfy such demands, hydrogels are one of the ideal candidates to protect bioactive molecules from degradation. Further, drug/protein delivery and release experiments can give information about perm-selectivity of membrane which is vital for cell and cell-based drug delivery studies. Since it is highly documented that diffusivity in hydrogel depends on both network and solute properties, this regulation can be achieved with control of permeability for bioactive molecule delivery.[28, 51, 67]

In this study, the next step was to understand the diffusion of BSA and GLP1 (9-37) from hydrogels having permeability gradients for determination of release behavior of solutes. Based on molecular weight and concentration, fractional release as a function of time (min) is represented in Figure 4.5a and b for BSA. All cases showed biphasic release: Burst release and slowing phase. As expected, higher molecular weight and lower concentration increased yielded higher release fraction. After 1920 min, hydrogels

formed with 20 kDa PEGDA molecular weight and 5% PEGDA concentration released 100% of BSA, whereas 84% of BSA was released from hydrogels formed with 20 kDa PEGDA molecular weight and 10% PEGDA concentration (Figure 4.5). These released fractions decreased to 73% and 67% for hydrogels formed with 10 kDa PEGDA molecular weight, 5% and 10% PEGDA concentrations, respectively (Figure 4.5). This is due to incomplete release resulting from reduction in mesh size and swelling ratio. Such incomplete releases were also observed in bulk PEG hydrogels, PLGA microsphere and poly(N-isopropylacrylamide) hydrogel systems due to entrapment in the network as in our case.[30, 97, 98] Also, as this hydrogel system has porosity gradient, high PEGDA content at lower molecular weight could reduce the number of the pores available for a molecule with hydrodynamic radius of ~3.56 nm (Table 3.1).

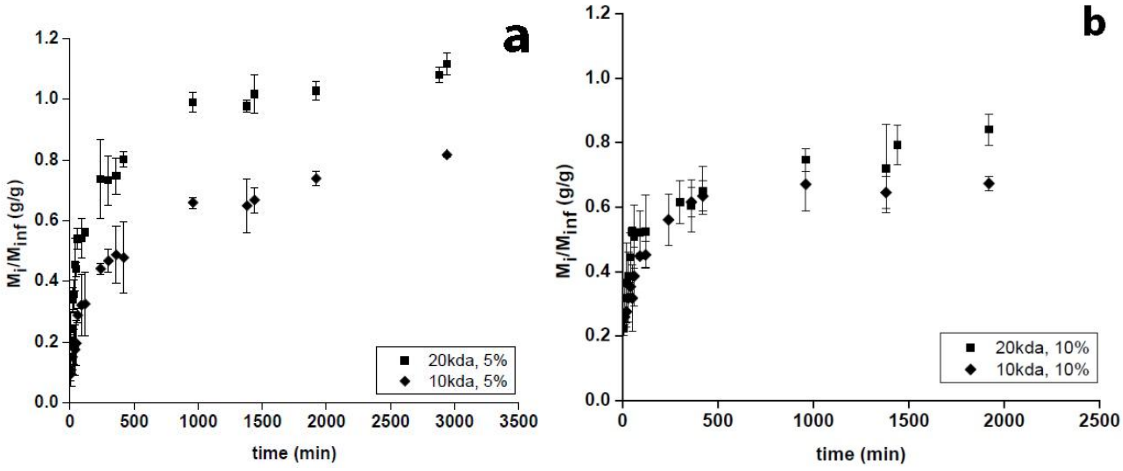

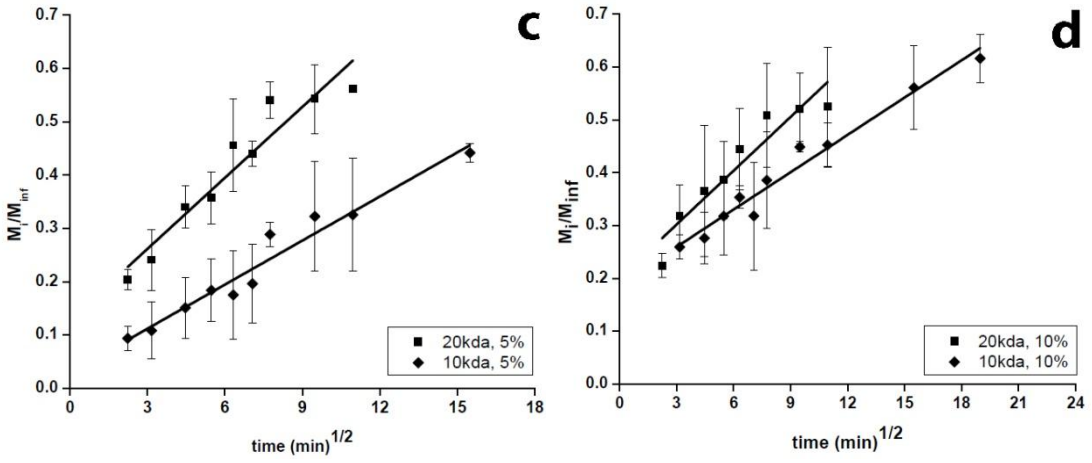

Figure 4.5. Fractional release of BSA from: a) and c) 20 kDa and 10 kDa, 5% PEG hydrogels, b) and d) 20 kDa and 10 kDa, 10% PEG hydrogels. Profiles in (c) and (d) represent the region where effective diffusivity calculations were carried out for hydrogels formed with 5 and 10% PEGDA concentration.

Although GLP1 (9-37) is a relatively small molecule with hydrodynamic radius of around ~1.3 nm compared to BSA (Table 3.1), the release profiles for GLP1 were similar to BSA. Burst release and nearly steady state regions were observed as in Figure 4.6a and 4.6b. Complete peptide release was observed at 180 min and 300 min through hydrogels formed with 20 kDa PEGDA molecular weight, 5% and 10% PEGDA concentrations, respectively. Decreasing PEGDA molecular weight from 20 kDa to 10 kDa retarded protein diffusion and complete release was observed after 300 and 660 min through hydrogels formed with 10 kDa PEGDA molecular weight, 5% and 10% PEGDA concentrations, respectively. In contrast to the releases observed for BSA, whole GLP-1 loaded was released from hydrogels depending on the network properties. For all conditions studied, 60 % of the GLP-1 peptide was released within less than 2 h (Figure 4.6). Although the results showed that the mesh size for all conditions were large enough for GLP-1 to pass through, the diffusion rate of this small molecule was still hindered similar to the condition observed for BSA.

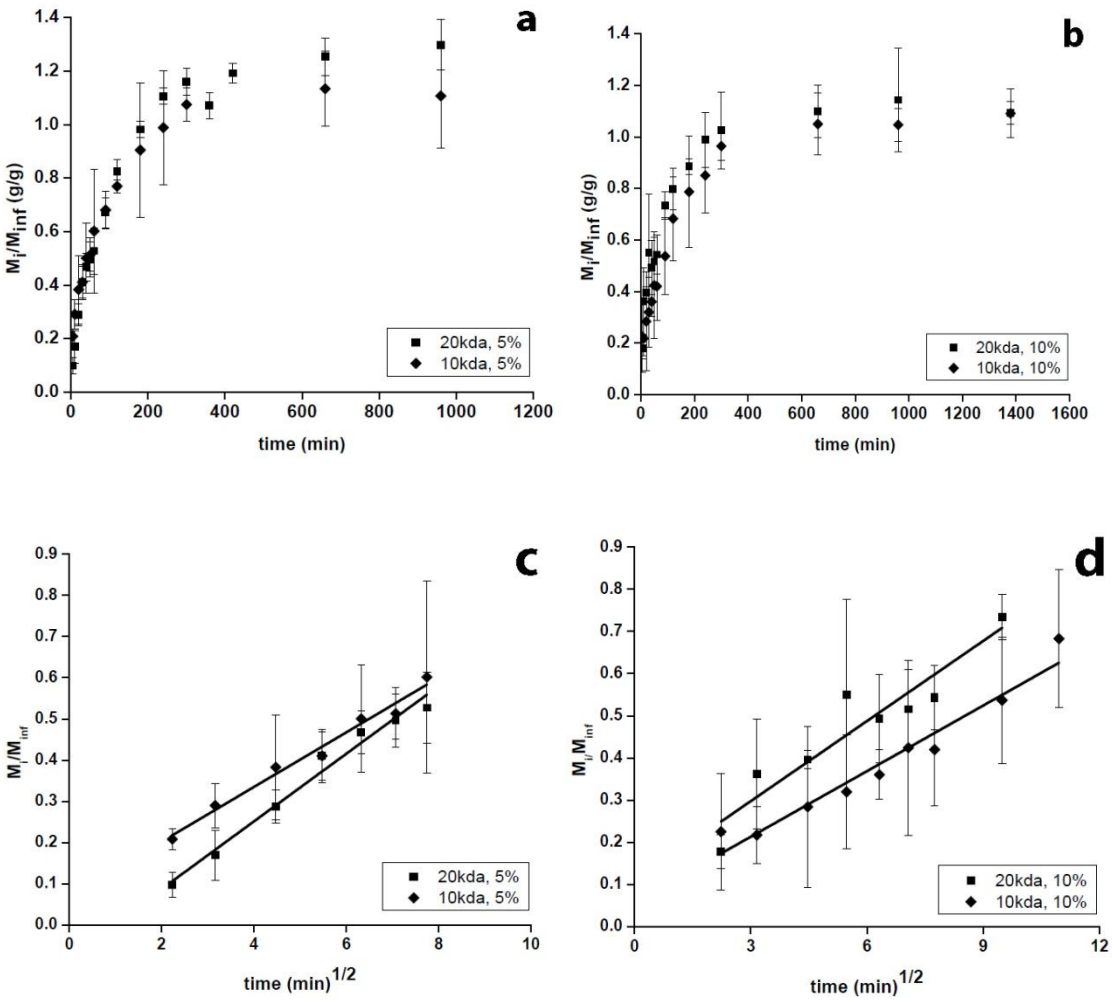

Figure 4.6. Fractional release of GLP1 (9-37) from: a) and c) 20 kDa and 10 kDa, 5% PEG hydrogels, b) and d) 20 kDa and 10 kDa, 10% PEG hydrogels. c) and d) represent the region where effective diffusivity calculation was carried out.

The results for both BSA and GLP1 (9-37) demonstrated that decrease in protein size and increase in molecular weight and concentration of crosslinker (in this case, PEGDA) enhanced release rate. Increasing molecular weight or decreasing concentration of PEGDA upregulates distance between crosslink junctions and results in higher swelling ratios (higher water content), in turn, these lead to larger pores and facilitates protein

diffusion. Smaller molecules diffused faster compared to larger ones, as larger ones needed more drag and larger pores to diffuse out.[9, 67]

4.2.2. Effective Diffusivities of BSA and GLP1 (9-37) Released from PEG Hydrogels

Diffusion coefficient is an important parameter which gives information about how fast a molecule can travel through a medium. In this study, BSA and GLP (9-37) were chosen to study release behaviour through PEG hydrogels, as this would be important for microencapsulated islets within PEG hydrogels studies. Such release profiles have been utilized to calculate effective diffusivities within the region $M_i/M_{inf}<0.6$ (Figure 4.5c, 4.5d, 4.6c and 4.6d) with modified Fick's law (Equation 3.10).

As expected, the slope of diffusion through hydrogels formed with 20 kDa PEGDA molecular weight and 5% PEGDA concentration was higher compared to the diffusion observed in hydrogels synthesized with other conditions, which is due to the presence of looser network structure, resulting in higher release late. For other conditions studied, at constant molecular weight or concentration increasing molecular weight or decreasing concentration yielded higher release rates (Figure 4.5c, 4.5d, 4.6c and 4.6d). Sixty percent of BSA was released from hydrogels synthesized with 20 kDa PEGDA molecular weight, 5% and 10% PEGDA concentrations at the end of 120 min. In contrast, increasing concentration or decreasing molecular weight resulted in prolonged diffusion rate. When hydrogels were formed with 10 kDa PEGDA and 5% and 10% PEGDA concentrations in the prepolymer, 60% of BSA was released into the medium within 240 and 360 min, respectively. For the case of GLP1 (9-37), the release of 60% was achieved at the end of 60 min for hydrogels formed with 20 kDa PEGDA molecular weight and 5% PEGDA concentration. Increasing concentration of PEGDA from 5% to 10% lead to 60% of total protein release within 90 min. When PEGDA molecular weight was reduced to 10 kDa,

and 5% and 10%, of PEGDA concentrations were used, the duration for 60% GLP-1 releases were measured as 60 min and 120 min, respectively. It should be noted that 60% of the solute was diffused out faster for GLP1 (9-37) compared to BSA from all PEG hydrogels studied.

Effective diffusivities for BSA calculated from Fick's law were ranging from 10^{-7} to 10^{-8} cm^2/s. Effective diffusivities were higher in 20 kDa PEG hydrogels than 10 kDa PEG hydrogels (Figure 4.7a). Diffusivity was calculated as $2.59X10^{-7}$ cm^2/s for the case of hydrogels formed with 20 kDa PEGDA molecular weight, and 5% PEGDA concentration. When the concentration of PEGDA was doubled and PEGDA molecular weight was kept constant, diffusivity was reduced to 60% of the value obtained at lower PEGDA concentration. For lower PEGDA molecular weight of 10 kDa, 5% PEGDA concentration in the prepolymer resulted in the diffusivity value of $9.93X10^{-8}$ cm^2/s for BSA. This was lowered to $7.3X10^{-8}$ cm^2/s for the diffusion of BSA through hydrogels formed with 10 kDa PEGDA molecular weight and 10% PEGDA concentration in the prepolymer.

In Figure 4.8a, the effects of molecular weight and concentration of PEGDA on diffusion of BSA is demonstrated in comparison with the diffusivity in water at 37°C. The results for BSA showed that the effective diffusivity was reduced to ~28% and ~17% of water for the diffusion through hydrogels synthesized with 20 kDa PEGDA, 5% and 10% PEGDA concentrations, respectively. These cases were lowered down to ~11% and ~7.9% of water for the diffusion through hydrogels synthesized with10 kDa PEGDA, 5% and 10% PEGDA concentrations, respectively.

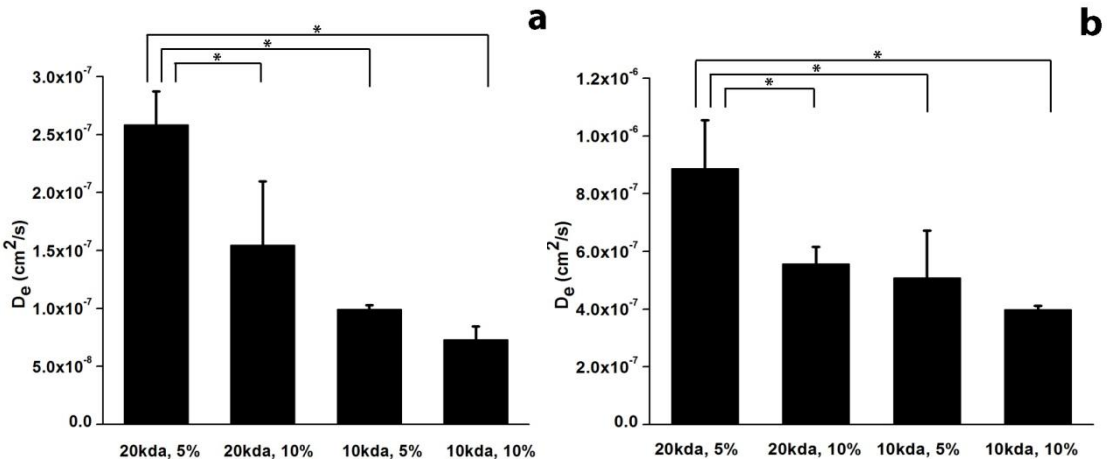

Figure 4.7. Effect of PEGDA molecular weight and concentration on diffusion coefficients of: a) BSA, b) GLP1 (9-37). Asterisk (*) indicates statistical significance.

As can be observed in Figure 4.7b, the effective diffusivity for GLP1 (9-37) was on the order of 10^{-7} cm^2/s for the diffusion through all hydrogels studied here. Similar to the results obtained for BSA release, hydrogels formed with 20 kDa PEGDA monomer resulted in higher effective diffusivities compared to the diffusivities obtained through hydrogels formed with10 kDa PEGDA monomer. Diffusivity of GLP1 (9-37) from 20 kDa, 5% PEG hydrogels was $8.9X10^{-7}$ cm^2/s. For 20 kDa 10% PEG hydrogels, effective diffusivity was $5.6X10^{-7}$ cm^2/s. When molecular weight of PEGDA in the prepolymer was reduced from 20 kDa to 10 kDa, the diffusivities through hydrogels were $5.1X10^{-7}$ cm^2/s and 4.0 cm^2/s for the case of 5% and 10% PEGDA monomer concentration, respectively.

Figure 4.8b illustrates that GLP1 (9-37) diffusion reduced to one order of magnitude compared to the values measured at diffusivity in water at 37°C. The release occurred at a diffusivity of ~35% of the value measured in water when hydrogels were formed with 20 kDa PEGDA and 5% PEGDA concentration. At constant PEGDA molecular weight, increasing the concentration of PEGDA from 5% to 10% resulted in lower diffusivities,

where ~22% of the water diffusivity was obtained. When hydrogels were synthesized with lower PEGDA molecular weight of 10 kDa, increasing the concentration of PEGDA from 5% to 10% decreased the effective diffusivity from ~20% to ~16% to that of the value measured in water.

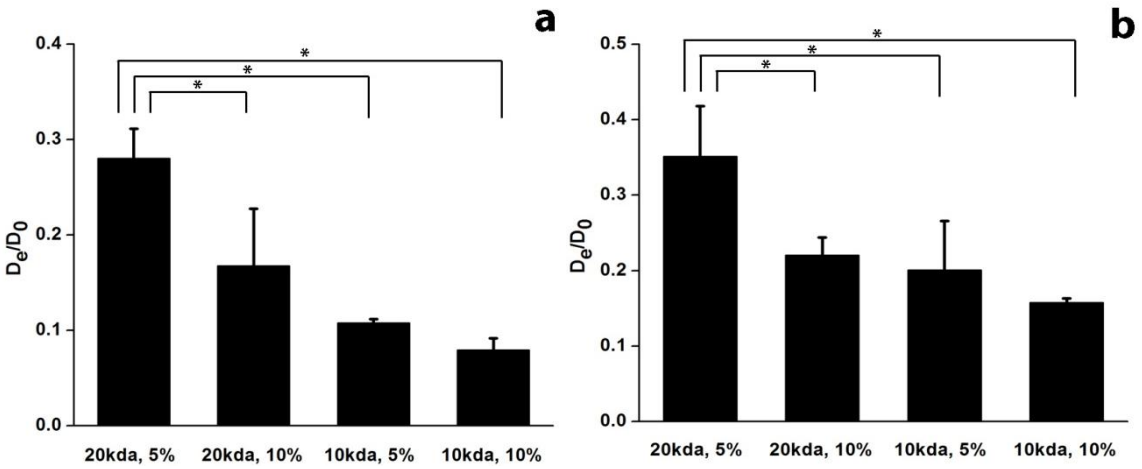

Figure 4.8. Normalized diffusion coefficients for: a) BSA, b) GLP1(9-37). Asterisk (*) indicates statistical significance.

As expected, the results showed that solute size has a significant effect on solute diffusion [67]: GLP1 (9-37) released faster than BSA. Further, it was showed that the network parameters such as crosslink density, M_c, swelling and pore size affect the diffusivity of the solute. Increases in M_c resulted in higher swelling and mesh size and such increases facilitated protein diffusion with higher diffusivity.[67] In contrast, crosslink density created negative effect on diffusion showing that increasing concentration or decreasing molecular weight reduced diffusivity.

Effective diffusivities calculated from equation 14, were shown to be PEGDA concentration and molecular weight dependent (Figure 4.6 and 4.7). Since higher PEG content at lower concentration has smaller pore size, it restricted the release of solute and

reduced effective diffusivity. The obstructions in the network composition can also interfere with solute diffusion. Slowly moving chains hinder diffusion by increasing the length of the path to move through. As observed, solute size had significant effect on diffusion. BSA diffusivity values were reduced more compared to the decreases observed for GLP1 (9-37) as a result of higher monomer concentration or lower monomer chain length. This is because, the network chains cause more drag force on higher sized solute due to increased hydrodynamic friction.[9, 36, 67, 70]

All results confirm that BSA and GLP1 (9-37) can be released in a controlled manner through PEG hydrogels studied here. In order to extend the duration of protein release monomer concentration or chain length could be tuned independently.

4.3. Viability of Fibroblasts Encapsulated within RGDS Functionalized/Nonfunctionalized PEG Hydrogels

For a biomaterial to be applicable in biomedical applications, it is well known that these materials should also be nontoxic and cytocompatible. In addition to semipermeability, biocompatibility is another factor to support cell viability in long terms for development of bioarficial organ.[92] For this reason, fibroblasts were encapsulated within naked and RGDS functionalized PEG hydrogels and viability was measured at day 1 and day 3. As demonstrated in Figure 4.9, the proposed system can support cell survival when RGDS incorporated. As expected, naked hydrogels could not support cells and this property caused significant decrease in cell viability as was measured by viability assay.

As illustrated in Figure 4.9, on day 3, fibroblast viability was increased by a factor of 1.31 compared to the viability observed at day 1 when PEG monomer conjugate including RGDS was added into the prepolymer. Similarly, there was 56% increase in

the viability of cells when PEGDA monomer concentration was doubled and PEGDA molecular weight was kept constant at 20 kDa. When lower PEGDA molecular weight was used (10 kDa) at 5% and 10% PEGDA concentrations were used, RGDS modified hydrogels increased viability 55% and 51% when compared to day 1. In contrast, all hydrogels formed without acr-PEG-RGDS conjugate could not support cell survival and significant reductions in viable cell number were observed. On day 3, 56% and 35% of fibroblasts were viable within 20 kDa, 5% and 10% PEG hydrogels, respectively. During the same incubation period, viable cell number decreased to 45% and 63% of day 1 in 10 kDa, 5% and 10% PEG hydrogels.

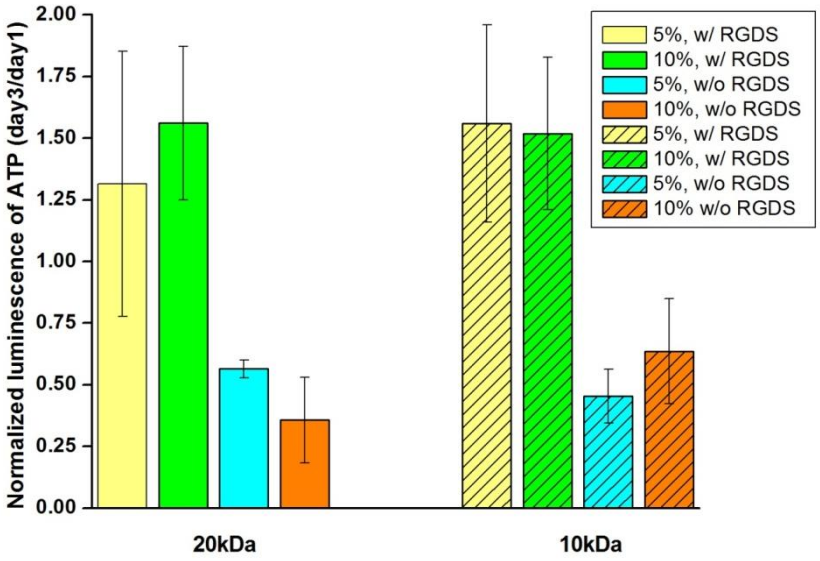

Figure 4.9. Viability of fibroblasts in PEG hydrogels represented as normalized ATP luminescence (day 3/day1). The group means of 20 kDa significantly differ from each other. Similarly, the group means of 10 kDa significantly differ from each other.

The covalent incorporation of RGDS resulted in promising cell viabilities when fibroblasts were encapsulated within these PEG hydrogel scaffolds, as hydrogels without this peptide were unable to support cell viability due to resistance of PEG to cell adhesion

(Figure 4.9).[7, 40] It is well established in the literature that RGDS promotes cell adhesion, which contributed to cell viability significantly. The results also showed that viability were nearly unaffected by network parameters. This demonstrates that PEG hydrogels generated in this study had large pores to allow diffusion of nutrients and other molecules and formation of free radicals during photopolymerization did not have negative effect on cell viability. Similar results were reported by Bott et al. showing that FXIII crosslinked PEG hydrogels can support human dermal fibroblast survival with incorporation of RGD.[15] In another study, Liao et al. indicated that increase in concentration or decrease in molecular weight enhanced proliferation rate of vocal fold fibroblasts in PEG hydrogels.[50] These nondegradable PEG hydrogels constructs can also support proliferation and survival of other cell types such as chondrocytes as was reported by Lin and her colleagues, where increasing molecular weight enhanced cell viability and survival of chondrocytes.[49]

Chapter 5

CONCLUSIONS

In tissue engineering and drug delivery, permeability gradients of surrounding membrane have profound effect on viability and functionality of cells/bioactive molecules. For this purpose, in this study, PEG hydrogels were generated via surface initiated photopolymerization with permeability gradients. Characterization was carried out with swelling and protein release experiments to determine the effect of permeability. The results confirmed that hydrogel mesh size can be regulated with molecular weight and concentration of backbone material and this type of hydrogels is applicable to controlled release of bioactive molecules. By using such hydrogels, permeability gradients can be formed in a single step efficiently. Controlled release of hormones and drug can be achieved and local delivery without side effects of bolus injection can come into reality. Further, encapsulation of NIH 3T3 fibroblasts proved that RGDS functionalized PEG hydrogels with permeability gradients are suitable tools for cell based studies. By gradient based distribution of proteins, synthetic biomaterials that mimic natural tissues can be created *in vitro* and detailed insight about cell-cell and cell-biomaterial interactions can be obtained with PEG hydrogels formed by surface initiated photopolymerization.

BIBLIOGRAPHY

1. Lowman, A.A. and N.A. Peppas, *Hydrogels*, in *Encyclopedia of Controlled Drug Delivery*, E. Mathiowitz, Editor 1999, John Wiley and Sons. p. 297-406.
2. Chen, R.R. and D.J. Mooney, *Polymeric growth factor delivery strategies for tissue engineering.* Pharm Res, 2003. **20**(8): p. 1103-12.
3. Hoffman, A.S., *Hydrogels for biomedical applications.* Adv Drug Deliv Rev, 2002. **54**(1): p. 3-12.
4. Gupta, P., V. Kavita, and G. Sanjay, *Hydrogels: from controlled release to pH-responsive drug delivery.* DDT, 2002. **7**: p. 569-578.
5. Sant, S., et al., *Biomimetic Gradient Hydrogels for Tissue Engineering.* Canadian Journal of Chemical Engineering, 2010. **88**(6): p. 899-911.
6. Kizilel, S., V.H. Perez-Luna, and F. Teymour, *Photopolymerization of poly(ethylene glycol) diacrylate on eosin-functionalized surfaces.* Langmuir, 2004. **20**(20): p. 8652-8.
7. Hacker, M.C. and A.G. Mikos, *Synthetic Polymers*, in *Principles of Regenerative Medicine*, A. Atala, et al., Editors. 2008, Academic Press: Canada. p. 604-635.
8. Cruise, G.M., D.S. Scharp, and J.A. Hubbell, *Characterization of permeability and network structure of interfacially photopolymerized poly(ethylene glycol) diacrylate hydrogels.* Biomaterials, 1998. **19**(14): p. 1287-94.
9. Zustiak, S.P. and J.B. Leach, *Characterization of protein release from hydrolytically degradable poly(ethylene glycol) hydrogels.* Biotechnol Bioeng, 2011. **108**(1): p. 197-206.
10. Weber, L.M., C.G. Lopez, and K.S. Anseth, *Effects of PEG hydrogel crosslinking density on protein diffusion and encapsulated islet survival and function.* J Biomed Mater Res A, 2009. **90**(3): p. 720-9.
11. Zisch, A.H., M.P. Lutolf, and J.A. Hubbell, *Biopolymeric delivery matrices for angiogenic growth factors.* Cardiovasc Pathol, 2003. **12**(6): p. 295-310.
12. Moon, J.J., et al., *Biomimetic hydrogels with pro-angiogenic properties.* Biomaterials, 2010. **31**(14): p. 3840-7.
13. Kizilel, S., M. Garfinkel, and E. Opara, *The bioartificial pancreas: progress and challenges.* Diabetes Technol Ther, 2005. **7**(6): p. 968-85.
14. Raeber, G.P., M.P. Lutolf, and J.A. Hubbell, *Part II: Fibroblasts preferentially migrate in the direction of principal strain.* Biomech Model Mechanobiol, 2008. **7**(3): p. 215-25.

15. Bott, K., et al., *The effect of matrix characteristics on fibroblast proliferation in 3D gels.* Biomaterials, 2010: p. 8454-64.
16. DeLong, S.A., A.S. Gobin, and J.L. West, *Covalent immobilization of RGDS on hydrogel surfaces to direct cell alignment and migration.* J Control Release, 2005. **109**(1-3): p. 139-48.
17. Nemir, S., H.N. Hayenga, and J.L. West, *PEGDA hydrogels with patterned elasticity: Novel tools for the study of cell response to substrate rigidity.* Biotechnol Bioeng, 2010. **105**(3): p. 636-44.
18. Schmidt, J.J., J. Rowley, and H.J. Kong, *Hydrogels used for cell-based drug delivery.* Journal of Biomedical Materials Research Part A, 2008. **87A**(4): p. 1113-1122.
19. Kizilel, S., *Mathematical Model for Microencapsulation of Pancreatic Islets within a Biofunctional PEG Hydrogel.* Macromolecular Theory and Simulations, 2010. **19**(8-9): p. 514-531.
20. Peppas, N.A. and A.R. Khare, *Preparation, structure and diffusional behavior of hydrogels in controlled release.* Adv Drug Deliv Rev, 1993. **11**: p. 1-35.
21. Lin, C.C. and A.T. Metters, *Hydrogels in controlled release formulations: network design and mathematical modeling.* Adv Drug Deliv Rev, 2006. **58**(12-13): p. 1379-408.
22. Zisch, A.H., et al., *Cell-demanded release of VEGF from synthetic, biointeractive cell ingrowth matrices for vascularized tissue growth.* FASEB J, 2003. **17**: p. 2260-2.
23. Kizilel, S., et al., *Sequential formation of covalently bonded hydrogel multilayers through surface initiated photopolymerization.* Biomaterials, 2006. **27**(8): p. 1209-15.
24. Silva, A.K., et al., *Growth factor delivery approaches in hydrogels.* Biomacromolecules, 2009. **10**(1): p. 9-18.
25. Kim, B.S. and D.J. Mooney, *Development of biocompatible synthetic extracellular matrices for tissue engineering.* Trends Biotechnol, 1998. **16**(5): p. 224-30.
26. Tibbitt, M.W. and K.S. Anseth, *Hydrogels as Extracellular Matrix Mimics for 3D Cell Culture.* Biotechnol Bioeng, 2009. **103**(4): p. 655-663.
27. Zavan, B., C. Roberta, and A. Giovanni, *Hydrogels and Tissue Engineering*, in *Hydrogels Biological Properties and Applications*, R. Barbucci, Editor, 2009, Springer: Italy. p. 1-8.
28. Hoare, T.R. and D.S. Kohare, *Hydrogels in drug delivery: progress and challenges.* polymer, 2008. **49**: p. 1993-2007.

29. Seliktar, D., et al., *MMP-2 sensitive, VEGF-bearing bioactive hydrogels for promotion of vascular healing.* Journal of Biomedical Materials Research Part A, 2004. **68**(4): p. 704-16.
30. Drapala, P.W., et al., *Role of Thermo-responsiveness and Poly(ethylene glycol) Diacrylate Cross-link Density on Protein Release from Poly(N-isopropylacrylamide) Hydrogels.* Journal of Biomaterials Science-Polymer Edition, 2011. **22**(1-3): p. 59-75.
31. Wang, C.M., R.R. Varshney, and D.A. Wang, *Therapeutic cell delivery and fate control in hydrogels and hydrogel hybrids.* Adv Drug Deliv Rev, 2010. **62**(7-8): p. 699-710.
32. Sreejalekshmi, K.G. and P.D. Nair, *Biomimeticity in tissue engineering scaffolds through synthetic peptide modifications-Altering chemistry for enhanced biological response.* Journal of Biomedical Materials Research Part A, 2011. **96A**(2): p. 477-491.
33. Burdick, J.A., et al., *Delivery of osteoinductive growth factors from degradable PEG hydrogels influences osteoblast differentiation and mineralization.* Journal of Controlled Release, 2002. **83**(1): p. 53-63.
34. Hennink, W.E. and C.F. van Nostrum, *Novel crosslinking methods to design hydrogels.* Adv Drug Deliv Rev, 2002. **54**(1): p. 13-36.
35. Deligkaris, K., et al., *Hydrogel-based devices for biomedical applications.* Sensors and Actuators B-Chemical, 2010. **147**(2): p. 765-774.
36. Nafea, E.H., et al., *Immunoisolating semi-permeable membranes for cell encapsulation: focus on hydrogels.* Journal of Controlled Release, 2011. **154**(2): p. 110-22.
37. Leslie-Barbick, J.E., J.J. Moon, and J.L. West, *Covalently-immobilized vascular endothelial growth factor promotes endothelial cell tubulogenesis in poly(ethylene glycol) diacrylate hydrogels.* J Biomater Sci Polym Ed, 2009. **20**(12): p. 1763-79.
38. Lee, K.Y. and S.H. Yuk, *Polymeric protein delivery systems.* Progress in Polymer Science, 2007. **32**(7): p. 669-697.
39. Zhu, J., *Bioactive modification of poly(ethylene glycol) hydrogels for tissue engineering.* Biomaterials, 2010. **31**: p. 4639-4656.
40. Veronese, F.M., A. Mero, and G. Pasut, *Protein PEGylation, Basic science and Biological Applications*, ed. F.M. Veronese2009, Switzerland: Birkhäuser Verlag.
41. Lin, C.C. and K.S. Anseth, *PEG hydrogels for the controlled release of biomolecules in regenerative medicine.* Pharm Res, 2009. **26**(3): p. 631-43.
42. Shalaby, S.W., *Biabsorbable Polymers*, in *Encyclopedia of Pharmaceutical Technology*, S. J., Editor 2006, Informa Healthcare.

43. Hern, D.L. and J.A. Hubbell, *Incorporation of adhesion peptides into nonadhesive hydrogels useful for tissue resurfacing.* J Biomed Mater Res, 1998. **39**(2): p. 266-276.
44. Mann, B.K., R.H. Schmedlen, and J.L. West, *Tethered-TGF-beta increases extracellular matrix production of vascular smooth muscle cells.* Biomaterials, 2001. **22**(5): p. 439-44.
45. Anderson, S.B., et al., *The performance of human mesenchymal stem cells encapsulated in cell-degradable polymer-peptide hydrogels.* Biomaterials, 2011. **32**(14): p. 3564-74.
46. Schmidt, J.J., J. Rowley, and H.J. Kong, *Hydrogels used for cell-based drug delivery.* J Biomed Mater Res A, 2008. **87**(4): p. 1113-22.
47. Bryant, S.J., et al., *Crosslinking density influences chondrocyte metabolism in dynamically loaded photocrosslinked poly(ethylene glycol) hydrogels.* Ann Biomed Eng, 2004. **32**: p. 407-417.
48. Nuttelman, C.R., M.C. Tripodi, and K.S. Anseth, *Synthetic hydrogel niches that promote hMSC viability.* Matrix Biology, 2005. **24**(3): p. 208-218.
49. Lin, S., et al., *Influence of physical properties of biomaterials on cellular behavior.* Pharm Res, 2011. **28**(6): p. 1422-30.
50. Liao, H., et al., *Influence of hydrogel mechanical properties and mesh size on vocal fold fibroblast extracellular matrix production and phenotype.* Acta Biomater, 2008. **4**(5): p. 1161-71.
51. Weber, L.M., C.G. Lopez, and K.S. Anseth, *Effects of PEG hydrogel crosslinking density on protein diffusion and encapsulated islet survival and function.* Journal of Biomedical Materials Research Part A, 2009. **90**(3): p. 720-9.
52. McCall, J.D., C.C. Lin, and K.S. Anseth, *Affinity Peptides Protect Transforming Growth Factor Beta During Encapsulation in Poly(ethylene glycol) Hydrogels.* Biomacromolecules, 2011. **12**(4): p. 1051-1057.
53. Siegel, R.A. and R. Langer, *Controlled Release of Polypeptides and Other Macromolecules.* Pharm Res, 1984(1): p. 2-10.
54. DeLong, S.A., A.S. Gobin, and J.L. West, *Covalent immobilization of RGDS on hydrogel surfaces to direct cell alignment and migration.* Journal of Controlled Release, 2005. **109**(1-3): p. 139-48.
55. Peret, B.J. and W.L. Murphy, *Controllable Soluble Protein Concentration Gradients in Hydrogel Networks.* Adv Funct Mater, 2008. **18**(21): p. 3410-3417.
56. Chatterjee, K., et al., *The effect of 3D hydrogel scaffold modulus on osteoblast differentiation and mineralization revealed by combinatorial screening.* Biomaterials, 2010. **31**(19): p. 5051-62.

57. Cruise, G.M., et al., *A sensitivity study of the key parameters in the interfacial photopolymerization of poly(ethylene glycol) diacrylate upon porcine islets.* Biotechnol Bioeng, 1998. **57**(6): p. 655-65.
58. Tsai, D.H., et al., *Adsorption and Conformation of Serum Albumin Protein on Gold Nanoparticles Investigated Using Dimensional Measurements and in Situ Spectroscopic Methods.* Langmuir, 2011.
59. Klajnert, B., et al., *Interactions between PAMAM dendrimers and bovine serum albumin.* Biochim Biophys Acta, 2003. **1648**(1-2): p. 115-26.
60. Teles, H., et al., *Hydrogels of collagen-inspired telechelic triblock copolymers for the sustained release of proteins.* J Control Release, 2010. **147**(2): p. 298-303.
61. Lee, S.H., et al., *Proteolytically degradable hydrogels with a fluorogenic substrate for studies of cellular proteolytic activity and migration.* Biotechnol Prog, 2005. **21**(6): p. 1736-41.
62. Leach, J.B. and C.E. Schmidt, *Characterization of protein release from photocrosslinkable hyaluronic acid-polyethylene glycol hydrogel tissue engineering scaffolds.* Biomaterials, 2005. **26**(2): p. 125-35.
63. Li, Y., et al., *PEGylated PLGA nanoparticles as protein carriers: synthesis, preparation and biodistribution in rats.* Journal of Controlled Release, 2001. **71**(2): p. 203-11.
64. Rothen-Weinhold, A., et al., *Release of BSA from poly(ortho ester) extruded thin strands.* Journal of Controlled Release, 2001. **71**(1): p. 31-7.
65. Leonard, M., et al., *Hydrophobically modified alginate hydrogels as protein carriers with specific controlled release properties.* Journal of Controlled Release, 2004. **98**(3): p. 395-405.
66. Xu, Y. and Y. Du, *Effect of molecular structure of chitosan on protein delivery properties of chitosan nanoparticles.* Int J Pharm, 2003. **250**(1): p. 215-26.
67. Engberg, K. and C.W. Frank, *Protein diffusion in photopolymerized poly(ethylene glycol) hydrogel networks.* Biomed Mater, 2011. **6**(5): p. 055006.
68. Drapala, P.W., et al., *Role of Thermo-responsiveness and Poly(ethylene glycol) Diacrylate Cross-link Density on Protein Release from Poly(N-isopropylacrylamide) Hydrogels.* J Biomater Sci Polym Ed, 2010.
69. Reinhart, C.T. and N.A. Peppas, *Solute diffusion in swollen membranes. Part II. influence of crosslinking on diffusive properties.* Journal of Membrane Science, 1984. **18**: p. 227-239.
70. Merrill, E.W., K.A. Dennison, and C. Sung, *Partitioning and diffusion of solutes in hydrogels of poly(ethylene oxide).* Biomaterials, 1993. **14**(15): p. 1117-26.
71. Vahl, T.P., et al., *Effects of GLP-1-(7-36)NH2, GLP-1-(7-37), and GLP-1- (9-36)NH2 on intravenous glucose tolerance and glucose-induced insulin secretion in healthy humans.* J Clin Endocrinol Metab, 2003. **88**(4): p. 1772-9.

72. Kizilel, S., et al., *Encapsulation of pancreatic islets within nano-thin functional polyethylene glycol coatings for enhanced insulin secretion.* Tissue Eng Part A, 2010. **16**(7): p. 2217-28.
73. Hersel, U., C. Dahmen, and H. Kessler, *RGD modified polymers: biomaterials for stimulated cell adhesion and beyond.* Biomaterials, 2003. **24**(24): p. 4385-415.
74. Dalton, S.L., E.E. Marcantonio, and R.K. Assoian, *Cell attachment controls fibronectin and alpha 5 beta 1 integrin levels in fibroblasts. Implications for anchorage-dependent and -independent growth.* J Biol Chem, 1992. **267**(12): p. 8186-91.
75. Massia, S.P. and J.A. Hubbell, *An RGD spacing of 440 nm is sufficient for integrin alpha V beta 3-mediated fibroblast spreading and 140 nm for focal contact and stress fiber formation.* J Cell Biol, 1991. **114**(5): p. 1089-100.
76. Rydholm, A.E., C.N. Bowman, and K.S. Anseth, *Degradable thiol-acrylate photopolymers: polymerization and degradation behavior of an in situ forming biomaterial.* Biomaterials, 2005. **26**(22): p. 4495-506.
77. Heutz, J.P.A., *Theory of Radical Reactions*, in *Handbook of Radical Polymerization*, K. Matyjaszewski and T.P. Davis, Editors. 2002, Wiley Interscience: Hoboken. p. 1-76.
78. Nguyen, K.T. and J.L. West, *Photopolymerizable hydrogels for tissue engineering applications.* Biomaterials, 2002. **23**(22): p. 4307-14.
79. Bryant, S.J. and K.S. Anseth, *Photopolymerization of Hydrogel Scaffolds*, in *Scaffolding in Tissue Engineering*, P.X. Ma and J.H. Elisseeff, Editors. 2006, CRC Press: US. p. 71-90.
80. Kizilel, S., V.H. Perez-Luna, and F. Teymour, *Modeling of PEG Hydrogel Membranes for Biomedical Applications.* Macromolecular Reaction Engineering, 2009. **3**(5-6): p. 271-287.
81. Carr, D.A. and N.A. Peppas, *Molecular structure of physiologically-responsive hydrogels controls diffusive behavior.* Macromol Biosci, 2009. **9**(5): p. 497-505.
82. Zustiak, S.P. and J.B. Leach, *Hydrolytically degradable poly(ethylene glycol) hydrogel scaffolds with tunable degradation and mechanical properties.* Biomacromolecules, 2010. **11**(5): p. 1348-57.
83. Peppas, N. and E.W. Merrill, *Determination of interaction parameter $\chi 1$, for poly(vinyl alcohol) and water in gels crosslinked from solutions.* Journal of Polymer Science: Polymer Chemistry, 1976. **14**(2): p. 459-464.
84. Canal, T. and N.A. Peppas, *Correlation between mesh size and equilibrium degree of swelling of polymeric networks.* J Biomed Mater Res, 1989. **23**(10): p. 1183-93.
85. Bird, R.B., W.E. Steward, and E.N. Lightfoot, *Transport Phenomena*. 2nd ed, 2007, USA: John Wiley and Sons, Inc.

86. Geankoplis, C.J., *Transport Processes and Separation Process Principles (Includes Unit Operations)*. 4th ed, 2003, USA: Prentice Hall.
87. Fox, C.B., et al., *Single-molecule fluorescence imaging of peptide binding to supported lipid bilayers.* Anal Chem, 2009. **81**(13): p. 5130-8.
88. Peppas, N.A., *Analysis of Fickian and non-Fickian drug release from polymers.* Pharm Acta Helv, 1985. **60**(4): p. 110-1.
89. Costa, P. and J.M. Sousa Lobo, *Modeling and comparison of dissolution profiles.* Eur J Pharm Sci, 2001. **13**(2): p. 123-33.
90. Siepmann, J. and F. Siepmann, *Mathematical modeling of drug delivery.* Int J Pharm, 2008. **364**(2): p. 328-43.
91. Zustiak, S.P., H. Boukari, and J.B. Leach, *Solute diffusion and interactions in cross-linked poly(ethylene glycol) hydrogels studied by Fluorescence Correlation Spectroscopy.* Soft Matter, 2010. **6**(15): p. 3609-3618.
92. Burczak, K., et al., *Protein permeation through poly(vinyl alcohol) hydrogel membranes.* Biomaterials, 1994. **15**(3): p. 231-8.
93. Martens, P. and K.S. Anseth, *Characterization of hydrogels formed from acrylate modified poly(vinyl alcohol) macromers.* Polymer, 2000. **41**(21): p. 7715-7722.
94. Davis, B.K., *Diffusion of polymer gel implants.* Proc Natl Acad Sci U S A, 1974. **71**(8): p. 3120-3.
95. Ju, H., et al., *Preparation and characterization of crosslinked poly(ethylene glycol) diacrylate hydrogels as fouling-resistant membrane coating materials.* Journal of Membrane Science, 2009. **330**(1-2): p. 180-188.
96. Ostroha, J.L., *PEG-based Degradable Networks for Drug Delivery Applications*, in *Materials Engineering*2006, Drexel University. p. 165.
97. Lin, C.C. and A.T. Metters, *Enhanced protein delivery from photopolymerized hydrogels using a pseudospecific metal chelating ligand.* Pharm Res, 2006. **23**(3): p. 614-22.
98. Duncan, G., et al., *The influence of protein solubilisation, conformation and size on the burst release from poly(lactide-co-glycolide) microspheres.* J Control Release, 2005. **110**(1): p. 34-48.
99. Wootton, T.P., et al., *Hydrology Handbook*. 2nded, 1996, US.
100. Crank, J., *The Mathematics of Diffusion*. 2nd ed, 1975, Great Britain: Oxford University Press.

APPENDIX

1. Permeability

Permeability is a property that is defined as the capability of a fluid or molecule to pass through (mass transfer) a porous matrix depending on matrix properties.[99] Mass transfer of a molecule depends on mass flux which is a function of concentration gradient and diffusivity.[86]

For porous medium, permeability can be calculated with Darcy's law:[86]

$$\upsilon' = -\frac{k}{\mu}\frac{\Delta p}{\Delta L} \qquad \text{(Equation A.1)}$$

where v' is the superficial velocity (cm/s), k is permeability (cm^2 cp/s.atm), μ is the viscosity (cp), Δp is pressure drop (atm) and ΔL is length (cm).[86]

2. Derivation of Modified Fick's Law

2.1. Derivation of Fick's law (for 1D diffusion)

Transport of a property by molecular movement depends on a driving force to overcome a process and can be expressed as:[86]

$$rate\ of\ a\ transfer\ process = \frac{driving\ force}{resistance} \qquad \text{(Equation A.2)}$$

The diffusion of a property can be expressed as in equation A.3 for steady state.

$$\psi_x = -\delta\frac{d\Gamma}{dx} \qquad \text{(Equation A.3)}$$

Here, Ψ_x is the flux of a property (amount of the property transferred per unit cross sectional area per time perpendicular to the x direction). Γ is the concentration of the property and δ is the proportionality constant known as diffusivity. [86]

For an unsteady state process, a general property balance is required for entire system as represented in equation A.4 and figure 1.

$$\begin{bmatrix} rate\ of \\ property\ in \end{bmatrix} + \begin{bmatrix} rate\ of\ generation \\ of\ property \end{bmatrix} = \begin{bmatrix} rate\ of \\ property\ out \end{bmatrix} + \begin{bmatrix} rate\ of\ accumulation \\ of\ property \end{bmatrix} \quad \text{(EquationA.4)}$$

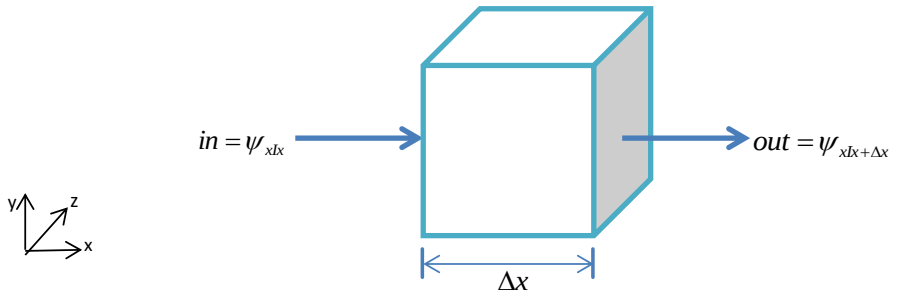

Figure 1. Unsteady state mass balance.

$$(\psi_{xIx}) \cdot \Delta y \Delta z + R(\Delta x \cdot \Delta y \Delta z) = (\psi_{xIx+\Delta x}) \cdot \Delta y \Delta z + \frac{\partial \Gamma}{\partial t}(\Delta x \cdot \Delta y \Delta z) \quad \text{(Equation A.5)}$$

Dividing by ΔxΔyΔz and letting Δz go to zero,

$$R = \frac{\partial \Psi_x}{\partial x} + \frac{\partial \Gamma}{\partial t} \quad \text{(Equation A.6)}$$

Substituting equation A.3 into equation A.6 results in:

$$R = \frac{\partial \Gamma}{\partial t} - \delta \frac{\partial^2 \Gamma}{\partial x^2} \quad \text{(Equation A.7)}$$

If there is no generation present in the system,

$$\frac{\partial \Gamma}{\partial t} = \delta \frac{\partial^2 \Gamma}{\partial x^2} \quad \text{(Equation A.8)}$$

Equation A.8 relates between the concentration of the property (Γ) to the distance x and time t. [86]

For mass diffusivity, equation A.3 is expressed as follows,

$$J_x = -D\frac{dc}{dx} \qquad \text{(Equation A.9)}$$

This equation is known as Fick's law of diffusion for molecular transport. Here, J_x is the flux in kg mol/s.m^2, D is the diffusion coefficient in m^2/s and c is the concentration in kg mol/m^3. It assumes that mass diffusivity is independent from concentration. [86]

Equation A.8 is represented as Fick's second law of diffusion for unsteady state as shown below: [86]

$$\frac{\partial c}{\partial t} = D\frac{\partial^2 c}{\partial x^2} \qquad \text{(Equation A.10)}$$

2. Derivation of Modified Fick's Law (Korsmeyer-Peppas)

Assuming that release experiments are carried out under perfect sink conditions, boundary conditions (Equations A.11 and A.12) shown below can be applied to solve Fick's second law of diffusion (Equation A.10). [62, 88]

$$t = 0 \qquad -\frac{\delta}{2} < x < \frac{\delta}{2} \qquad c = c_0 \qquad \text{(Equation A.11)}$$

$$t > 0 \qquad x = \pm\frac{\delta}{2} \qquad c = c_1 \qquad \text{(Equation A.12)}$$

Here, c_0 is the initial concentration; c_1 is the external concentration at the interface and can be taken as zero.

The exact solution of equation A.10 under boundary conditions gives the following result:[100]

$$\frac{M_i}{M_{\inf}} = 4\left(\frac{Dt}{\delta^2}\right)^{1/2}\left\{\ \pi^{-1/2} + 2\sum_{n=1}^{\infty}(-1)^n ierfc\,\frac{n\delta}{2\sqrt{Dt}}\ \right\} \quad \text{(Equation A.13)}$$

In equation A.13, M_i and M_{inf} are the masses released at time i and infinity. D is the diffusion coefficient (effective), δ is the hydrogel thickness and t is time. [62, 88]

For the short release times in the region of $M_i/M_{inf}<0.6$, the right term inside the brackets vanishes and following equation is obtained.[62, 88]

$$\frac{M_i}{M_{\inf}} \cong 4\left(\frac{Dt}{\pi\delta^2}\right)^{1/2} \quad \text{(Equation A.14)}$$

VITA

Tuğba Bal was born in Istanbul, Turkey in 1988. Tuğba completed her Bachelor of Science degree with the highest honor in Molecular Biology and Genetics from Istanbul Technical University in 2010. She started her graduate school education in Chemical and Biological Engineering in Koç University in 2010. Her research interests are cell behavior within hydrogels, vascularization and bioactive molecule delivery.